

Nucleophilic Addition to the η^2 -Alkyne Ligand in $[\text{CpFe}(\text{CO})_2(\eta^2\text{-R-C}\equiv\text{C-R})]^+$. Dependence of the Alkenyl Product Stereochemistry on the Basicity of the Nucleophile

Munetaka Akita,* Satoshi Kakuta, Shuichiro Sugimoto, Masako Terada, Masako Tanaka, and Yoshihiko Moro-oka

Chemical Resources Laboratory, Tokyo Institute of Technology, 4259 Nagatsuta, Midori-ku, Yokohama 226-8503, Japan

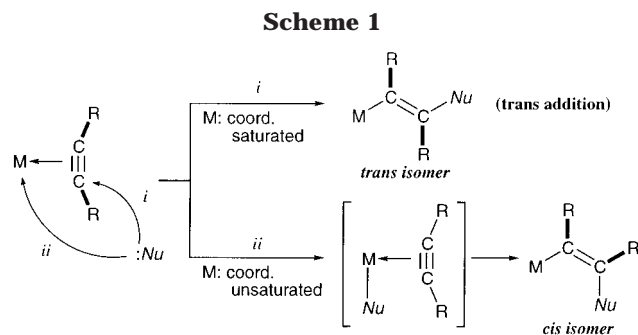
Received February 7, 2001

Reaction of the cationic η^2 -alkyne iron complex, $[\text{Fp}(\eta^2\text{-Ph-C}\equiv\text{CPh})\text{BF}_4$ (**1**) [$\text{Fp} = (\eta^5\text{-C}_5\text{H}_5)\text{-Fe}(\text{CO})_2$], with various *O*-, *N*-, and *C*-nucleophiles afforded products containing the $\text{Ph-C}=\text{C-Ph}$ linkage. i.e., *cis*- (**3**) and *trans*-alkenyl complexes (**4**), $\text{Fp-C}(\text{Ph})=\text{C}(\text{Ph})\text{-Nu}$, and metallacycles, $\text{Cp}(\text{CO})\text{Fe-C}(\text{Ph})=\text{C}(\text{Ph})\text{-C(=O)-Nu}$ [coordinated at =O (**5**) or *Nu* (**6**)]. Crystallographic determination of the configuration of the $\text{C}=\text{C}$ moiety in **3** and **4** and analysis of the product distribution revealed that basic nucleophiles bearing alkyl substituents produced the *cis*-alkenyl complex (**3**) and/or the metallacycles (**5**, **6**), whereas less basic nucleophiles bearing aryl substituents afforded the *trans*-alkenyl complex (**4**). Correlation between the product distribution and $\text{p}K_b$ values of the nucleophiles leads to the conclusions that (1) products **3**, **5**, and **6** arise from acyl intermediates formed by initial nucleophilic addition of basic nucleophiles at the CO ligand, (2) *trans*-alkenyl complexes **4** result from addition of less basic nucleophiles to the η^2 -alkyne ligand from the *exo*-side, and (3) the equilibrium of the CO addition governed by the basicity of the nucleophile is the key step of the diversity of the stereochemistry of the alkenyl products. Reactions of 2-hexyne complex, $[\text{Fp}(\eta^2\text{-Et-C}\equiv\text{C-Et})\text{BF}_4$ (**2**), were also examined.

Introduction

Nucleophilic addition to unsaturated substrates coordinated to a transition metal center is involved as a key step of various stoichiometric and catalytic transformations of hydrocarbons mediated by organometallic species.¹ As for nucleophilic addition to η^2 -alkyne complexes (Scheme 1),^{2,3} previous studies have led to the conclusion that *trans*-alkenyl complexes are obtained via addition from the side opposite of M when the metal center is coordinatively saturated (path *i*),² and contrary to this, the reaction of coordinatively unsaturated complexes may form *cis*-alkenyl complexes via initial addition to M followed by migration to the alkyne ligand (path *ii*),⁴ though the latter type of reactions similar to hydrometalation and carbometalation⁵ has not been studied in detail.

As a typical example of the *trans*-addition reaction, the extensive work done by Reger and co-workers can be raised (Scheme 2).^{2a} They examined reactions of a



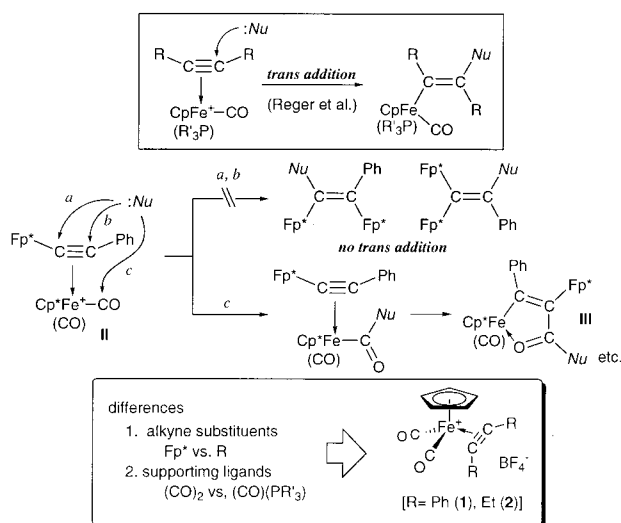
series of cationic η^2 -alkyne complexes, $[\text{CpFe}(\text{CO})(\text{L})(\eta^2\text{-R-C}\equiv\text{C-R})]^+$ [$\text{L} = \text{PR}'_3$, $\text{P}(\text{OR}'_3)_3$], with a variety

(1) Pearson, A. J. *Metalloorganic Chemistry*; Wiley-Interscience: New York, 1985. Yamamoto, A. *Organotransition Metal Chemistry*; Wiley-Interscience: New York, 1986. Collman, J. P.; Hegedus, L. S.; Norton, J. R.; Finke, R. G. *Principles and Applications of Organotransition Metal Chemistry*; University Science Books: Mill Valley, 1987. Cornils, B.; Herrmann, W.; *Applied Homogeneous Catalysis with Organometallic Compounds* (2 vols.); VCH: Oxford, 1996. Crabtree, R. H. *The Organometallic Chemistry of the Transition Metals*, 3rd ed.; Wiley-Interscience: New York, 2001.

(2) (a) Reger, D. L. *Acc. Chem. Res.* **1988**, *21*, 229, and references therein. (b) Reger, D. L.; Belmore, K. A.; Atwood, J. L.; Hunter, W. E. *J. Am. Chem. Soc.* **1983**, *105*, 5710. (c) Reger, D. L.; Klaeren, Stephen A.; Babin, J. E.; Adams, R. D. *Organometallics* **1988**, *7*, 181.

(3) Ru: (a) de Klerk-Engels, B.; Delis, Jos G. P.; Vrieze, K.; Goubitz, K.; Fraanje, J. *Organometallics* **1994**, *13*, 3269. Pd, Pt: (b) Cacchi, S. *J. Organomet. Chem.* **1999**, *576*, 42. (c) Yamamoto, Y.; Radhakrishnan, U. *Chem. Soc. Rev.* **1999**, *28*, 199. (d) Hewertson, W.; Taylor, I. C. *J. Chem. Soc. D* **1970**, 428. (e) Appleton, T. G.; Chisholm, M. H.; Clark, H. C.; Yasufuku, K. *J. Am. Chem. Soc.* **1974**, *96*, 6600. (f) Maassarani, F. Pfeffer, M.; Spencer, J.; Wehman, E. *J. Organomet. Chem.* **1994**, *466*, 265. (g) Dupont, J.; Casagrande, O. L., Jr.; Aiub, A. C.; Beck, J.; Hoerner, M.; Bortoluzzi, A. *Polyhedron* **1994**, *13*, 2583. (h) Dupont, J.; Basso, N. R.; Meneghetti, M. R.; Konrath, R. A.; Burrow, R.; Horner, M. *Organometallics* **1997**, *16*, 2386. Mo: (i) Davidson, J. L.; Murray, I. E. P.; Preston, P. N.; Russo, Maria, V.; Manojlovic-Muir, L.; Muir, K. W. *J. Chem. Soc., Chem. Commun.* **1981**, 1059. (j) Davidson, J. L.; Vasapollo, G.; Manojlovic-Muir, L.; Muir, K. W. *J. Chem. Soc., Chem. Commun.* **1982**, 1025. (k) Feng, S. G.; White, P. S.; Templeton, J. L. *J. Am. Chem. Soc.* **1990**, *112*, 8192. Polymetallic compounds: (l) Aime, S.; Deeming, A. J. *J. Chem. Soc., Dalton Trans.* **1983**, 1807. (m) Cherkas, A. A.; Carty, A. J.; Sappa, E.; Pellinghelli, M. A.; Tiripicchio, A. *Inorg. Chem.* **1987**, *26*, 3201. (n) Breimair, J.; Steimann, M.; Wagner, B.; Beck, W. *Chem. Ber.* **1990**, *123*, 7. (o) Cherkas, A. A.; Breckenridge, S. M.; Carty, A. J. *Polyhedron* **1992**, *11*, 1075.

Scheme 2



of nucleophiles (*Nu*) giving *trans*-alkenyl complexes, $\text{CpFe}(\text{CO})(\text{L})-\text{C}(\text{R})=\text{C}(\text{R})-\text{Nu}$. As a result of a systematic study with the aid of crystallographic structure determination, the *trans*-addition rule (path *i* in Scheme 1) was established for the nucleophilic addition. The only exception was addition to the Cp ring leading to ring-substituted alkenyl complexes,^{2b} but *cis*-addition was not observed at all. However, configuration of tri- and tetrasubstituted alkenes resulting from the nucleophilic addition cannot be determined definitely by spectroscopic analysis alone. In later studies, therefore, when the configuration cannot be determined by the spectroscopic data, the *trans*-addition rule has been applied to assign the configuration.

We have been studying structure and reactivity of cationic dinuclear bridging acetylide complexes, $[\text{Fp}^*_{2-(\mu-\text{C}\equiv\text{C}-\text{R})}]\text{BF}_4$ [R = H (**I**), Ph (**II**); $\text{Fp}^* = (\eta^5\text{-C}_5\text{Me}_5)\text{-Fe}(\text{CO})_2$], and it was found that they exhibited divergent chemical properties depending on the substituent R.⁶ For example, they showed different reactivity toward nucleophiles. Reaction of **I** resulted in deprotonation to give the ethynediyl complex $\text{Fp}^*-\text{C}\equiv\text{C}-\text{Fp}^*$,^{6c,k} whereas addition reaction was observed for **II** (Scheme 2).^{6c,d} The addition reaction, however, did not afford a dimetalated alkene, which we expected on the basis of the *trans*-addition rule, but the products with the acyl functional group such as **III**, which should result from initial nucleophilic addition to the CO ligand (path *c*) instead of that to the η^2 -alkyne ligand (path *a* or *b*). The different initial reaction sites [CO (**II**) vs C≡C (Reger's system)] might be ascribed to (i) the alkyne substituent (Fp^*) in **II**, which would cause various types of influence on the electronic properties of the alkyne moiety, and/or (ii) the different auxiliary ligands [(CO)₂ vs (CO)-

(PR'₃)]. To make clear these effects, nucleophilic addition reaction to a simple mononuclear η^2 -alkyne complex containing the $[\text{CpFe}(\text{CO})_2]^+$ (Fp^+) fragment, $[\text{Fp}^+(\eta^2\text{-Ph-C}\equiv\text{C-Ph})]\text{BF}_4$ (**1**), was examined. As a result, reaction with amines and an alkanethiolate produced *cis*-alkenyl complexes, as we reported in the previous communication (see also text),^{6e} and we concluded that point (ii) was the crucial factor that determined the initial reaction site; in other words, initial addition to CO might lead to *cis*-addition. However, further study has revealed that reaction of **1** with various nucleophiles do not always produce *cis*-alkenyl complexes. Herein we disclose details of nucleophilic addition to cationic η^2 -alkyne iron complexes, $[\text{Fp}^+(\eta^2\text{-Ph-C}\equiv\text{C-Ph})]\text{BF}_4$ (**1**) and $[\text{Fp}^+(\eta^2\text{-Et-C}\equiv\text{C-Et})]\text{BF}_4$ (**2**), and the present study reveals factors determining initial nucleophilic addition sites (e.g., stereochemistry of the alkenyl products), which are dependent on the basicity (nucleophilicity) of the nucleophiles.

Results

Synthesis and Structural Characterization of Cationic η^2 -Alkyne Iron Complexes, $[\text{Fp}^+(\eta^2\text{-Ph-C}\equiv\text{C-Ph})]\text{BF}_4$ (1**) and $[\text{Fp}^+(\eta^2\text{-Et-C}\equiv\text{C-Et})]\text{BF}_4$ (**2**).** The cationic iron complexes with diphenylacetylene (**1**) and 3-hexyne ligand (**2**) used in the present study were prepared by substitution reaction of the labile precursor, $[\text{Fp}^+(\text{isobutene})]\text{BF}_4$, with appropriate alkynes according to the reported procedure.⁷ Their molecular structures were determined by X-ray crystallography. ORTEP views are shown in Figures 1 and 2, and selected structural parameters are summarized in Table 1. Details will be discussed later.

Reaction of $[\text{Fp}^+(\eta^2\text{-Ph-C}\equiv\text{C-Ph})]\text{BF}_4$ (1**) with Nucleophiles with Alkyl Substituents (HNR₂, NaOMe, NaSR) Giving *cis*-Alkenyl Complexes and/or Metallacycles.** Reaction of **1** with amines in $\text{CH}_2\text{-Cl}_2$ afforded two types of products containing the Ph-C=C-Ph linkage, i.e., Fp-alkenyl complex **3**, showing two $\nu(\text{CO})$ vibrations, and/or metallacycle **5**, showing only one $\nu(\text{CO})$ vibration (eq 1).⁸ In addition to these products, Fp_2 was occasionally formed as a minor byproduct. The spectroscopic data of **3** (Tables S1 and S2)⁹ are consistent with alkenyl complexes, $\text{Fp}-\text{C}(\text{Ph})=\text{C}(\text{Ph})-\text{Nu}$, which arise from nucleophilic addition of amines to the C≡C moiety. Configuration of the C=C

(4) Bottrill, M.; Green, M. *J. Am. Chem. Soc.* **1977**, *99*, 5795. Allen, S. R.; Baker, P. K.; Barnes, S. G.; Bottrill, M.; Green, M.; Orpen, A. G. *J. Chem. Soc., Dalton Trans.* **1983**, 927.

(5) (a) Negishi, E. *Pure Appl. Chem.* **1981**, *53*, 2333. Negishi, E.; Takahashi, T. *J. Synth. Org. Chem. Jpn.* **1989**, *47*, 2. (b) Asao, N.; Yamamoto, Y. *Chem. Rev.* **1993**, *93*, 2207. (c) Knochel, P. In *Comprehensive Organometallic Chemistry II*; Abel, E. W., Stone, F. G. A., Wilkinson, G., Eds.; Pergamon: Oxford, 1995; Vol. 11, p 159. (d) Negishi, E.; Kondakov, D. Y. *Chem. Soc. Rev.* **1996**, *25*, 417. (e) Marek, I.; Normant, J. F. *Transition Metal Org. Synth.* **1998**, *1*, 514. (f) Marek, I.; Normant, J. F. In *Metal-Catalyzed Cross-Coupling Reactions*; Diederich, F., Stang, P. J., Eds.; Wiley-VCH: Weinheim, 1998; p 271. (g) Asao, N.; Yamamoto, Y. *Bull. Chem. Soc. Jpn.* **2000**, *73*, 1071.

(6) (a) Akita, M.; Moro-oka, Y. *Bull. Chem. Soc. Jpn.* **1995**, *68*, 420. (b) Akita, M.; Terada, M.; Oyama, S.; Moro-oka, Y. *Organometallics* **1990**, *9*, 816. (c) Akita, M.; Terada, M.; Oyama, S.; Sugimoto, S.; Moro-oka, Y. *Organometallics* **1991**, *10*, 1561. (d) Akita, M.; Terada, M.; Moro-oka, Y. *Organometallics* **1991**, *10*, 2961. The reaction mechanism was corrected in ref 6h. (e) Akita, M.; Kakuta, S.; Sugimoto, S.; Terada, M.; Moro-oka, Y. *J. Chem. Soc., Chem. Commun.* **1992**, 451. (f) Akita, M.; Sugimoto, S.; Terada, M.; Moro-oka, Y. *J. Organomet. Chem.* **1993**, *447*, 103. (g) Akita, M.; Ishii, N.; Takabuchi, A.; Tanaka, M.; Moro-oka, Y. *Organometallics* **1994**, *13*, 258. (h) Akita, M.; Takabuchi, A.; Terada, M.; Ishii, N.; Tanaka, M.; Moro-oka, Y. *Organometallics* **1994**, *13*, 2516. (i) Terada, M.; Masaki, Y.; Tanaka, M.; Akita, M.; Moro-oka, Y. *J. Chem. Soc., Chem. Commun.* **1995**, 1611. (j) Akita, M.; Kato, S.; Terada, M.; Masaki, Y.; Tanaka, M.; Moro-oka, Y. *Organometallics* **1997**, *16*, 2392. (k) Akita, M.; Chung, M.-C.; Sakurai, A.; Sugimoto, S.; Terada, M.; Tanaka, M.; Moro-oka, Y. *Organometallics* **1997**, *16*, 4882. (l) Akita, M.; Sugimoto, S.; Hirakawa, H.; Kato, S.; Terada, M.; Tanaka, M.; Moro-oka, Y. *Organometallics* **2001**, *20*, in press. For recent related works, see: (m) Akita, M.; Chung, M.-C.; Sakurai, A.; Moro-oka, Y. *J. Chem. Soc., Chem. Commun.* **2000**, 1285, and references therein.

(7) Samuels, S.-B.; Berryhill, S. R.; Rosenblum, M. *J. Organomet. Chem.* **1979**, *166*, C9.

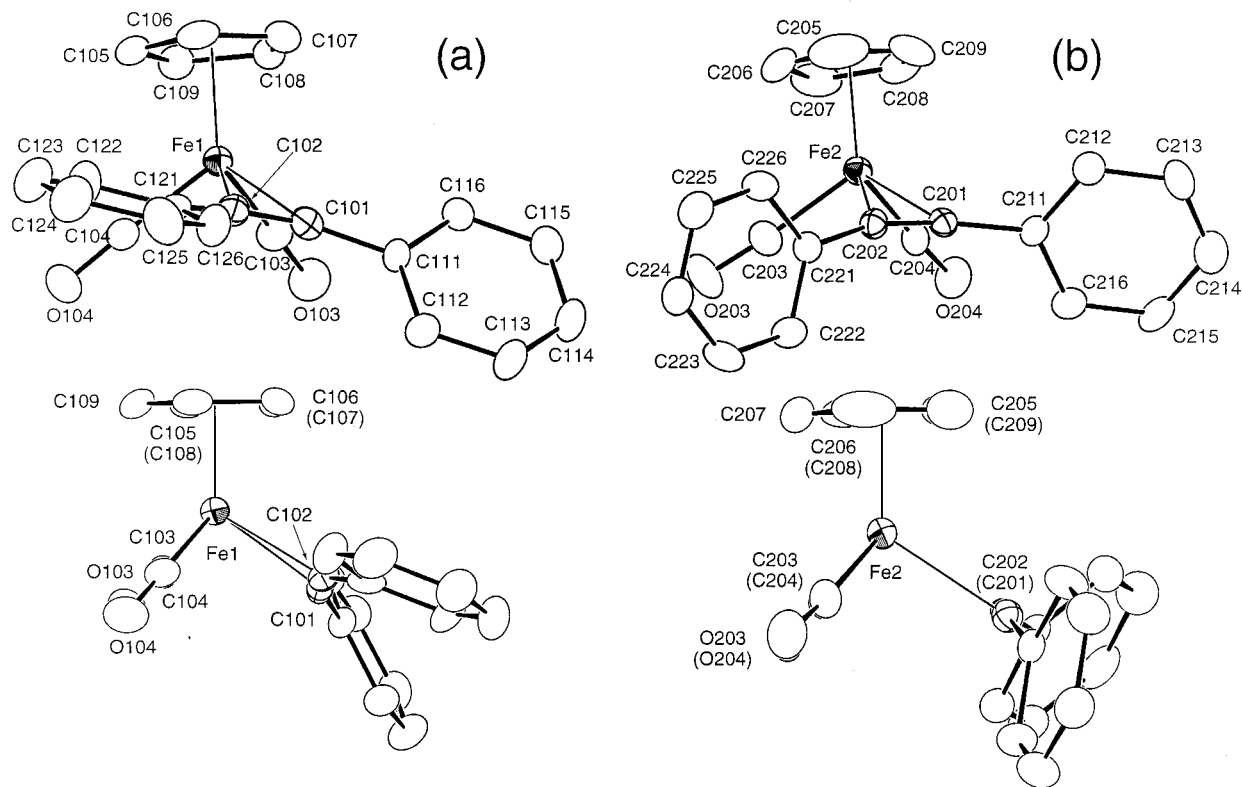


Figure 1. Molecular structure of the cationic part of **1** drawn at the 30% probability level: (a) molecule 1; (b) molecule 2.

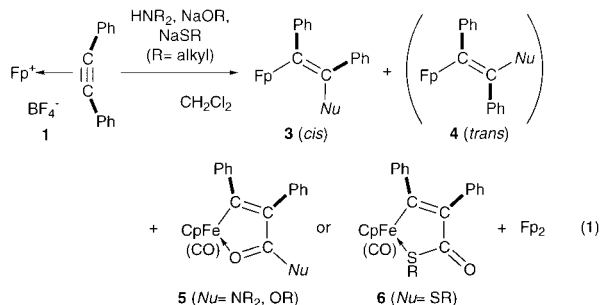
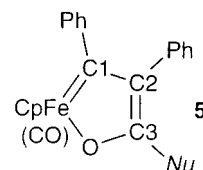


Chart 1



entry	Nu	reagent	pK _b ^b	yields (%)			
				3	5 (6)	Fp ₂	total
1	NHPr ^d (a)	H ₂ NPr ^d	3.40	0	45 (5a)	3	59 ^c
2	NHPr ^d (b)	H ₂ NPr ^d	3.29	0	39 (5b)	5	52 ^c
3	NHBu ^d (c)	H ₂ NBu ^d	3.32	0	13 (5c)	6	67 ^{c,d}
4	NEt ₂ (d)	H ₂ NEt ₂	2.98	61 (3d)	0	0	61
5	NPr ₂ (e)	HNPPr ₂ ^d	2.95	74 (3e) ^e	0	0	74
6	c-N(CH ₂) ₄ (f)	pyrrolidine	2.73	0	39 (5f) ^e	8	47
7	c-N(CH ₂) ₅ (g)	piperidine	2.77	71 (3g)	0	0	71
8	OMe (h)	NaOMe	-1.5	0	27 (5h)	10	48 ^c
9	OEt (i)	NaOEt	-1.9	0	74 (5i)	7	88 ^c
10	SEt (j)	NaSEt	3.39	56 (3j)	19 (6j)	4	79
11	SBu ^d (k)	NaSBu ^d	2.87	55 (3k) ^e	21 (6k)	14	90

^a determined by ¹H-NMR. ^b ref. 8. ^c Unidentified products (<10% yield) were also formed. ^d Adduct 3c⁺ (48%) was formed (see text). ^e characterized by X-ray crystallography.

bond of the NPr₂ derivative (**3e**) was determined to be *cis* as revealed by X-ray crystallography (Figure 3). The structural parameters of **3e** summarized in Table 2 fall in the accepted ranges, with the exception of the slightly bent Fe1–C4–O4 linkage [168(1)°]. This is presumably due to interaction with the lone pair electrons of N1, which is directed toward C4 with the separation of 2.69(1) Å. Because only one isomer each of the Fp–C(Ph)=C(Ph)–Nu-type alkenyl complexes was detected

by ¹H NMR analysis of the reaction mixtures (entries 4, 5, and 7), the alkenyl complexes **3d,g** were assigned to *cis*-structure **3**. The other product **5**, with a single ν(CO) vibration and a deshielded ¹³C NMR signal (δ_C 220–230), was assigned to the metallacyclic structure, which was confirmed for the Bu^dNH (**5c**)⁹ and pyrrolidinyl derivatives (**5f**, Figure 4) by X-ray crystallography. The deshielded ¹³C NMR signal should be ascribed to the contribution of another resonance structure **5'**, containing the carbenic Fe=C_α moiety (Chart 1).¹⁰ In accord with this description, the Fe1–C1 distances [1.947(4) Å (**5c**) and 1.946(7) Å (**5f**)] are substantially shorter than those in the alkenyl complexes **3** and **4** obtained by this study [Fe–C: 1.989–2.103 Å], and the C2–C3 lengths [1.463(6) Å (**5c**) and 1.465(8) Å (**5f**)] are also shorter than the corresponding bond lengths in the

(8) (a) **a**, **c–g**, **n–p**, **r**, **w**: Lide, D. R., Ed. *Handbook of Chemistry and Physics*, 76th ed.; CRC Press: Boca Raton, FL, 1995. (b) **j**, **m**, **q**, **t**: Dean, J. A., Ed. *Lange's Handbook of Chemistry*, 12th ed.; McGraw-Hill: New York, 1985. (c) **b**, **h**, **i**: Riddick, J. A.; Bunger, W. B.; Sakano, T. K. *Organic Solvents: Physical Properties and Methods of Purification*, 4th ed.; Wiley-Interscience: New York, 1986. (d) **k**: Yabroff, D. L. *Ind. Eng. Chem.* **1940**, *32*, 258. (e) **s**: Birchall, J. M.; Haszeldin, R. N. *J. Chem. Soc.* **1959**, 3653. (f) **u**: Bordwell, F. G.; Anderson, H. M. *J. Am. Chem. Soc.* **1953**, *75*, 6019. (g) Refs 8a,b,d,e, pK_b values in aqueous solutions; ref 8f, pK_b value in 48% EtOH aqueous solution.

(9) See Supporting Information.

(10) Mann, B. F.; Taylor, B. F. *¹³C NMR Data for Organometallic Compounds*; Academic Press: New York, 1981.

Table 1. Selected Structural Parameters for $[\text{Fp}^+(\eta^2\text{-R-C}\equiv\text{C-R})]\text{BF}_4$ [R = Ph (1), Et (2)]

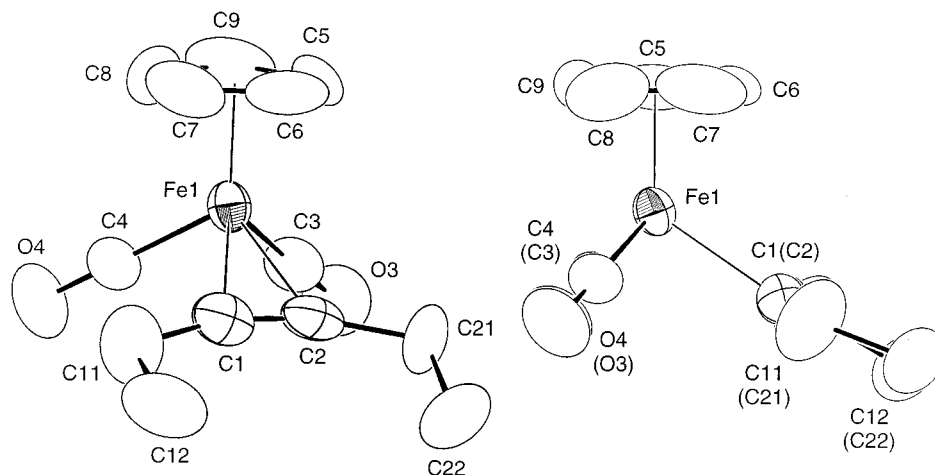
1 (Ph)				$[\text{CpFe}(\text{CO})[\text{P}(\text{OPh})_3](\eta^2\text{-Me-C}\equiv\text{C-R})]^+{}^a$			
molecule 1		molecule 2		2 (R = Et)		R = Me	R = Ph
Interatomic Distances (in Å)							
Fe1–C101	2.154(8)	Fe2–C201	2.16(1)	Fe1–C1	2.207(10)	2.165(7)	2.14(1)
Fe1–C102	2.116(9)	Fe2–C202	2.20(1)	Fe1–C2	2.20(1)	2.114(6)	2.146(9)
Fe1–C103	1.77(1)	Fe2–C203	1.796(9)	Fe1–C3	1.77(1)	1.796(8)	1.78(1)
Fe1–C104	1.79(1)	Fe2–C204	1.79(1)	Fe1–C4	1.77(1)	2.155(2) ^b	2.162(2) ^b
C101–C102	1.24(2)	C201–C202	1.22(1)	C1–C2	1.26(2)	1.19(1)	1.21(1)
C101–C111	1.44(1)	C201–C211	1.45(1)	C1–C11	1.50(2)	1.47(1)	1.49(1)
C102–C121	1.44(2)	C202–C221	1.44(1)	C2–C21	1.52(2)	1.49(1)	1.44(1)
C103–O103	1.15(2)	C203–O203	1.12(1)	C3–O3	1.13(1)	1.12(1)	1.12(2)
C104–O104	1.15(1)	C204–O204	1.14(1)	C4–O4	1.13(1)		
Fe1–C105–109	2.08–2.11(1)	Fe2–C205–209	2.04–2.08(2)	Fe1–C5–9	2.02–2.10(2)		
Bond Angles (in deg)							
C101–Fe1–C102	33.9(4)	C201–Fe2–C202	32.4(3)	C1–Fe1–C2	33.2(4)	32.4(3)	32.8(4)
Fe1–C101–C102	71.4(6)	Fe2–C201–C202	75.5(7)	Fe1–C1–C2	73.0(6)		
Fe1–C101–C111	130.6(7)	Fe2–C201–C211	125.0(6)	Fe1–C1–C11	125.9(8)		
C102–C101–C111	157.8(9)	C202–C201–C211	159(1)	C2–C1–C11	161(1)	157.7(7)	155(2)
Fe1–C102–C101	74.8(6)	Fe2–C202–C201	72.2(7)	Fe1–C2–C1	73.8(7)		
Fe1–C102–C121	132.3(6)	Fe2–C202–C221	126.7(8)	Fe1–C2–C21	123.1(7)		
C101–C102–C121	152.3(9)	C201–C202–C221	169(1)	C1–C2–C21	163(1)	158.4(8)	159(1)
Fe1–C103–O103	177.9(8)	Fe2–C203–O203	176(1)	Fe1–C3–O3	178.4(8)	175.3(7)	175.9(8)
Fe1–C104–O104	176(1)	Fe2–C204–O204	176.1(8)	Fe1–C4–O4	177(1)		

^a Corresponding parameters are shown. See ref 21. ^b P–C distances.

Table 2. Selected Structural Parameters for Alkenyl Complexes (3, 4, and 13) and Metallacycles (5 and 14)^a

complex ^b	Nu (reagent)	C1–C2	Fe1–C1	C2–Nu	Fe1–C1–C2	C1–C2–Nu
3e^c (<i>cis</i>)	NPr ⁱ ₂ (HNPr ⁱ ₂)	1.38(1)	1.989(7)	1.45(1)	127.9(7)	120.7(9)
3k^c (<i>cis</i>)	SBU ^t (NaSBU ^t)	1.30(1)	2.024(8)	1.790(7)	127.5(6)	121.7(6)
3z^c (<i>cis</i>)	C ₆ H ₂ Bu ^{1/2} OH (C ₆ H ₃ Bu ^{1/2} ONa)	1.338(5)	2.046(4)	1.513(5)	126.9(3)	124.7(3)
4l^c (<i>trans</i>)	OC ₆ H ₄ OPh- <i>p</i> (NaOC ₆ H ₄ OPh- <i>p</i>)	1.331(3)	2.031(2)	1.447(3)	125.5(2)	116.7(2)
4o^c (<i>trans</i>)	OC ₆ H ₄ Me- <i>p</i> (NaOC ₆ H ₄ Me- <i>p</i>)	1.25(1)	2.06(1)	1.46(1)	126.3(8)	118.7(9)
4q^c (<i>trans</i>)	OC ₆ H ₄ F- <i>p</i> (NaOC ₆ H ₄ F- <i>p</i>)	1.330(4)	2.021(3)	1.429(3)	128.6(2)	119.2(3)
4s^c (<i>trans</i>)	OC ₆ F ₅ (NaOC ₆ F ₅)	1.291(5)	2.026(4)	1.436(4)	128.1(3)	119.9(4)
4t^c (<i>trans</i>)	SPh (NaSPh)	1.244(9)	2.059(8)	1.812(8)	129.2(8)	121.7(8)
4v^c (<i>trans</i>)	N ₃ (NaN ₃)	1.354(7)	2.019(5)	1.446(6)	125.6(4)	117.6(4)
4w^c (<i>trans</i>)	OC(=O)Ph (NaOC(=O)Ph)	1.312(4)	2.034(3)	1.451(4)	126.1(2)	117.7(3)
4y^c (<i>trans</i>)	CH ₂ C(=O)Ph (CH ₂ =C(OSiMe ₃)Ph)	1.27(2)	2.01(1)	1.59(2)	124(1)	125(2)
5c^c (<i>trans</i>)	NHBU ^t (NH ₂ Bu ^t)	1.354(6)	1.947(4)		115.7(3)	
5f^c (cycle)	<i>c</i> -N(CH ₂) ₄ (pyrrolidine)	1.359(8)	1.946(7)		114.6(5)	
13f^c (<i>trans</i>)	OC ₆ H ₄ Me- <i>p</i> (NaOC ₆ H ₄ Me- <i>p</i>)	1.28(2)	2.15(2)	1.36(2)	128(1)	118(2)
14i^c (cycle)	SEt (NaSEt)	1.363(3)	1.938(7)		114.5(2)	

^a Bond lengths in Å and bond angles in deg. ^b Structures are shown in parentheses. ^c Obtained from **1**. ^d Obtained from **2**.

**Figure 2.** Molecular structure of the cationic part of **2** drawn at the 30% probability level.

acyclic =C-CO structure [cf. 1.499(7) Å for *trans*-Fp–C(Ph)=C(Ph)–COOMe,¹¹ 1.478(3) Å for *Z*-Fp–C(Ph)=CHCOOMe].^{6c}

(11) Kakuta, S.; Akita, M. Unpublished results.

A remarkable change in the product distribution is observed depending on the structure of amines, as can be seen from eq 1. In general, primary amines tend to produce metallacycle **5**, whereas secondary amines give *cis*-alkenyl complexes **3**. Reaction with a compact

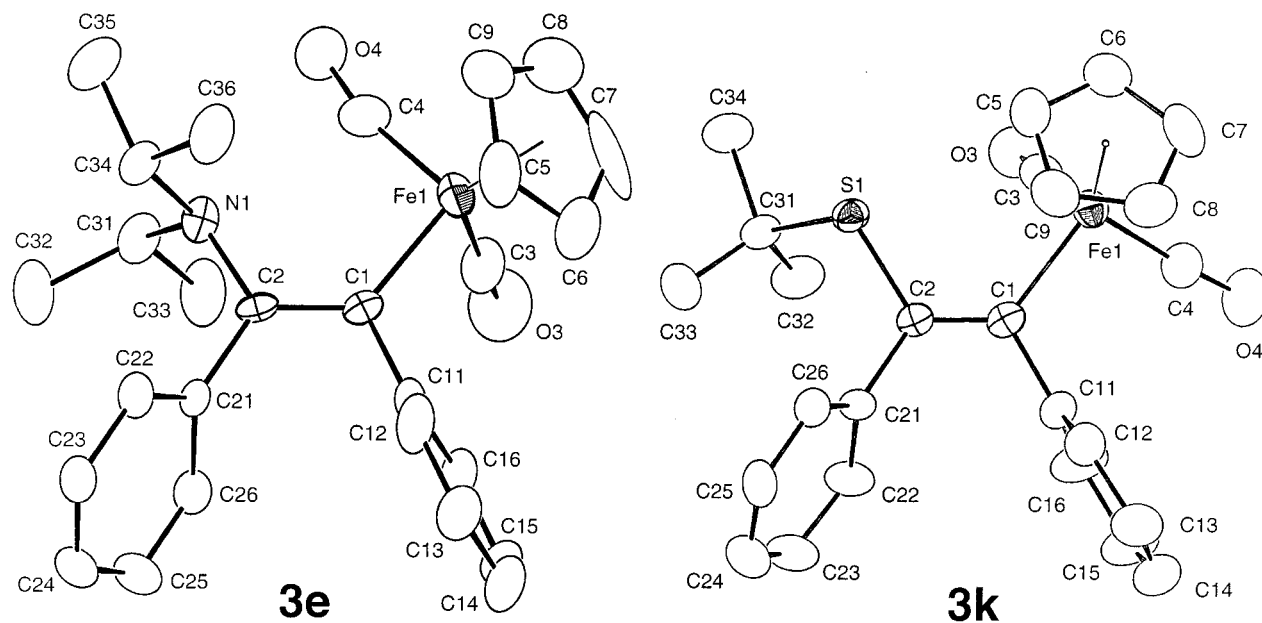


Figure 3. Molecular structures of *cis*-alkenyl complexes **3e** and **3k** drawn at the 30% probability level.

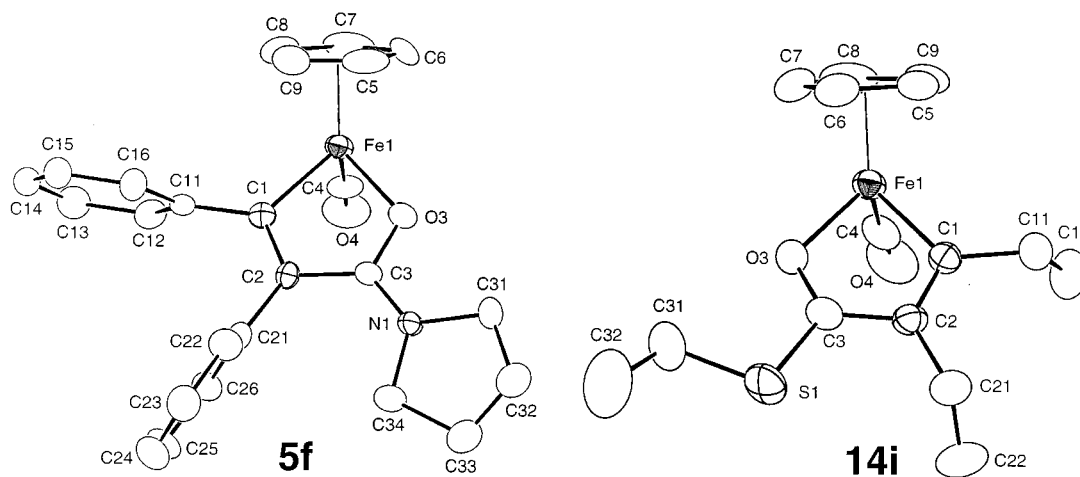
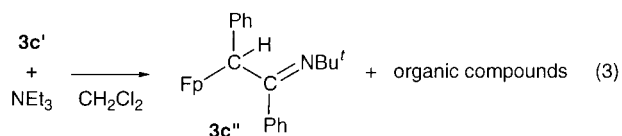
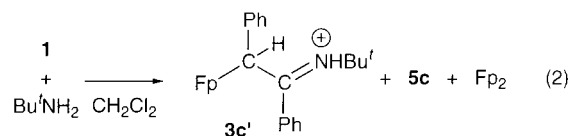


Figure 4. Molecular structure of metallacycles **5f** and **14i** drawn at the 30% probability level.

cyclic secondary amine (pyrrolidine; entry 6), however, produces the metallacycle **5f** in contrast to those with acyclic secondary amines mentioned above (entries 4, 5, and 7).

In the case of the reaction with $\text{Bu}'\text{NH}_2$, a different type of adduct **3c'** was obtained together with **5c** (eq 2). X-ray crystallography of **3c'** revealed the cationic



iminium ion structure (Figure 5 and Table 3) resulting from addition of $\text{H}-\text{NHBu}'$ across the $\text{C}\equiv\text{C}$ bond. The $\text{C}1-\text{C}2$ length [1.453(7) Å] falls in the range of $\text{C}(\text{sp}^3)-\text{C}(\text{sp}^2)$ single bonds, and the sp^3 -hybridized α -carbon

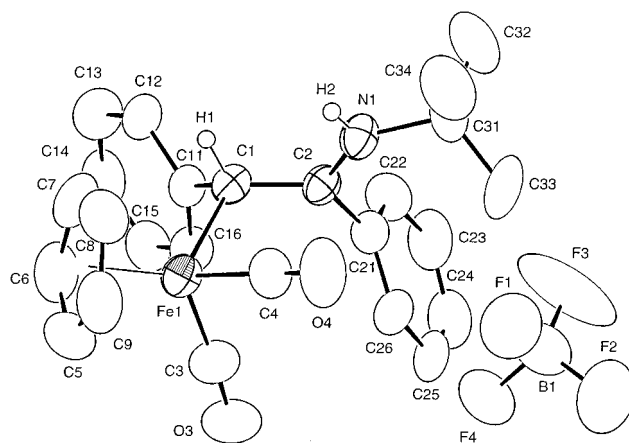


Figure 5. Molecular structure of **3c'** drawn at the 30% probability level.

atom (C1) is pyramidalized judging from the bond angles around it [110.8(4)–118.2(5)°; sum 340.3°, average: 113.4°]. In accord with this structure, its IR spectrum contains ν_{NH} (3261 cm^{-1}), ν_{CO} (2021, 1969 cm^{-1}), and ν_{BF} absorptions (1084 cm^{-1}), and its ^1H NMR

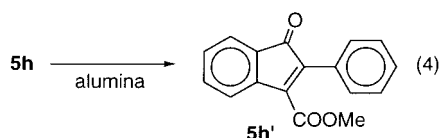
Table 3. Selected Structural Parameters for **3c'**

Bond Lengths (in Å)			
Fe1–C1	2.152(6)	N1–C2	1.301(7)
Fe1–C3	1.749(9)	N1–C31	1.515(8)
Fe1–C4	1.790(7)	C1–C2	1.453(7)
Fe1–C5–9	2.058(8)–2.109(7)	C1–C11	1.510(7)
O3–C3	1.144(8)	C2–C21	1.471(8)
O4–C4	1.118(7)		
Bond Angles (in deg)			
C1–Fe1–C3	97.9(3)	C2–C1–C11	118.2(5)
C1–Fe1–C4	93.3(3)	N1–C2–C1	117.1(6)
C3–Fe1–C4	94.2(4)	N1–C2–C21	120.5(6)
C2–N1–C31	135.2(6)	C1–C2–C21	122.3(6)
Fe1–C1–C2	111.3(4)	Fe1–C3–O3	175.6(8)
Fe1–C1–C11	110.8(4)	Fe1–C4–O4	175.6(7)

spectrum contains two broad signals (δ_{H} 5.35, 10.70), which are assigned to the α -CH and NH moieties, respectively. The former assignment was made based on a CH-HETCOR (COSY) spectrum,¹² in which the δ_{H} 5.35 signal was correlated to the sp^3 -carbon signal at δ_{C} 31.1 (d, $J_{\text{CH}} = 128$ Hz). The iminium salt **3c'** should be formed via nucleophilic addition of Bu^tNH_2 followed by H-transfer from N to the α -carbon atom in the resulting ammonioalkenyl intermediate $[\text{Fp}-\text{C}(\text{Ph})=\text{C}(\text{Ph})-\text{NH}_2\text{Bu}^t]^+$. To examine whether deprotonation of the iminium species **3c'** leads to alkenyl complex **3** or **4**, an isolated sample of **3c'** was treated with bases stronger than Bu^tNH_2 such as NEt_3 and 1,8-bis(dimethylamino)naphthalene (proton sponge) (eq 3). As a result, deprotonation of the NH moiety led to the formation of unstable imine complex **3c''** accompanying decomposed organic compounds. Retention of the α -CH moiety was supported by its NMR data [δ_{H} 4.03 (1H, s); δ_{C} 38.1 (d, $J = 134$ Hz)] close to those of **3c'**, and the loss of the NH proton is confirmed by (1) disappearance of the spectral features due to the NH group (δ_{H} , ν_{NH}) and (2) appearance of a $\nu_{\text{C}=\text{N}}$ vibration (1673 cm^{-1}). Thus the formation of **3c'** turned out to be an event independent from formation of alkenyl complexes.

Nucleophilic addition of an alkoxide anion to **1** resulted in the selective formation of metallacycles **5h,i**, which were characterized on the basis of a single $\nu(\text{CO})$ vibration and a deshielded C_α signal as observed for **5f** (eq 1). No trace of alkenyl complex was detected by ^1H NMR experiments. Although reaction with KOBU^t was also examined to see effects caused by a bulky substituent as observed for the reaction with amines, no adduct but Fp_2 was obtained as the sole organometallic product.

Let us note that metallacycle **5h**^{6e} obtained by the reaction with NaOMe decomposed during chromatographic separation to give indenone derivative **5h'**, which was characterized by spectroscopic and crystallographic analyses (eq 4).⁹ In another experiment treat-



ment of an isolated sample of **5h** with alumina (overnight in CH_2Cl_2) gave **5h'**. The formation of **5h'** could

(12) Akitt, J. W.; Mann, B. E. *NMR and Chemistry, An Introduction to Modern NMR Spectroscopy*, 4th ed.; Stanley Thorns: Cheltenham, 2000; p 290.

be explained in terms of a mechanism involving (1) decoordination of the $\text{C}=\text{O}$ group to form the coordinatively unsaturated species, (2) *cis* \rightarrow *trans* isomerization of the alkenyl moiety, (3) $\text{C}-\text{H}$ activation of the Ph group, and (4) reductive elimination, but no experimental support has been obtained. To our surprise, the indenone derivative was formed only from the MeO derivative **5h**, and no analogous product was obtained from the reactions with NaOEt and other nucleophiles described in this paper.

Reaction with alkanethiolates gave a mixture of three products: alkenyl complex **3**, metallacycle **5**, and Fp_2 (eq 1). Although a single isomer of the alkenyl complex **3** was detected by ^1H NMR monitoring of reaction mixtures, chromatographic separation caused isomerization, giving a mixture of alkenyl complexes **3j,k** and **4j,k**. In the case of the reaction with NaSEt , $\text{Fp}-\text{SEt}$ was also isolated from the reaction mixture. The kinetic product of the alkenyl complexes obtained by the reaction with NaSBu^t proved to be the *cis*-isomer **3k** as revealed by X-ray crystallography (Figure 3). Although the metallacycles **6j,k** showed ^{13}C NMR and IR features similar to those of **5** [(1) deshielded C_α signal and (2) single $\nu(\text{CO})$ vibration], the additional $\nu(\text{C}=\text{O})$ vibration observed around 1670 cm^{-1} led to the assignment to another cyclic structure **6**, where the highly polarizable sulfur atom is coordinated to the iron center instead of the $\text{C}=\text{O}$ functional group as in **5**.

Thus reaction of **1** with *N*-, *O*-, and *S*-nucleophiles bearing alkyl substituents afforded alkenyl complex **3** and metallacycles **5** and **6** containing the *cis*- $\text{Ph}-\text{C}=\text{C}-\text{Ph}$ linkage, and *trans*-isomer **4** was not formed at all. To our knowledge, this type of nucleophilic *cis*-addition reaction to a coordinatively saturated η^2 -alkyne complex has no precedent. To see the scope and limitation of the present unusual *cis*-addition reaction, reactions with various nucleophiles were next studied.

Reaction of $[\text{Fp}^+(\eta^2\text{-Ph}-\text{C}\equiv\text{C}-\text{Ph})]\text{BF}_4$ (1**) with Nucleophiles with Aryl Substituents (NaOAr , NaSAr) Giving *trans*-Alkenyl Complexes and/or Metallacycles.** As an extension of the above nucleophilic addition reactions, reaction with nucleophiles bearing aryl substituents was studied. Because reaction with aniline derivatives did not afford the expected alkenyl complex but substituted products such as $[\text{Fp}(\text{NH}_2\text{Ph})]\text{BF}_4$, the substituent effect was examined in detail for the *O*- and *S*-nucleophiles.

Reaction with various phenolate derivatives also produced alkenyl complex **4** and/or metallacycle **5** (eq 5). Product distribution determined by ^1H NMR is summarized in the table in eq 5. In sharp contrast to the *cis*-addition reaction with the alkyl-substituted nucleophiles, the configuration of the $\text{C}=\text{C}$ bond in **4** was *trans*, as revealed by X-ray crystallography of some of the reaction products, **4l**, **4o**, **4q**, and **4s**. As a typical example, the molecular structure of the *p*-methylphenoxy derivative **4o** is shown in Figure 6, and ORTEP views of the other products are included in Supporting Information.

Reaction with arenethiolates resulted in the exclusive formation of alkenyl complexes **4t,u**, which were isolated in good yields (eq 6), and the configuration of the

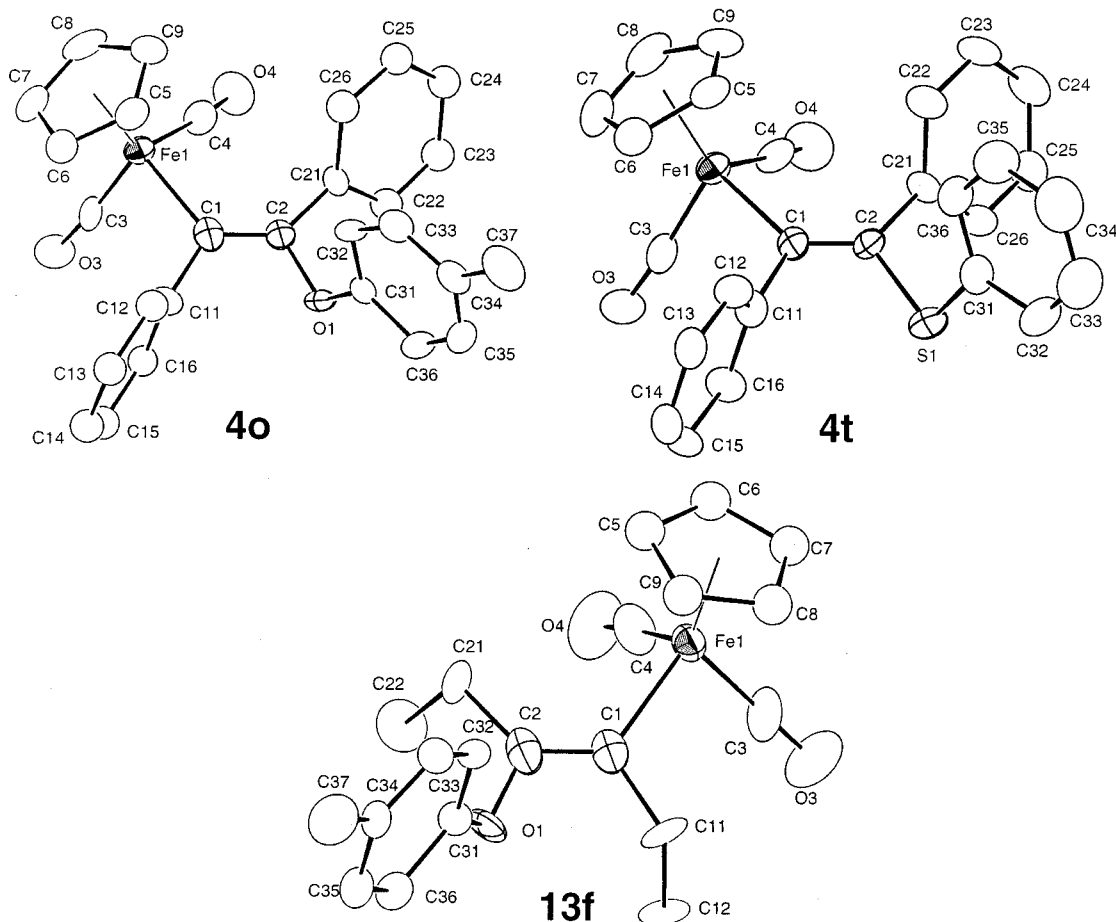
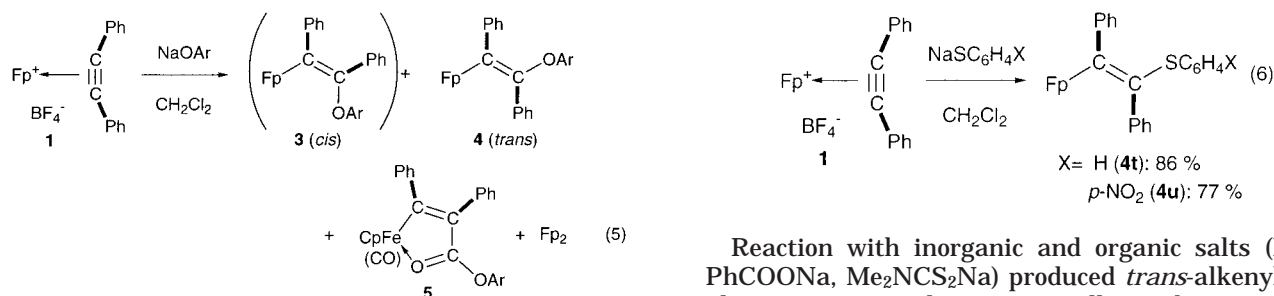
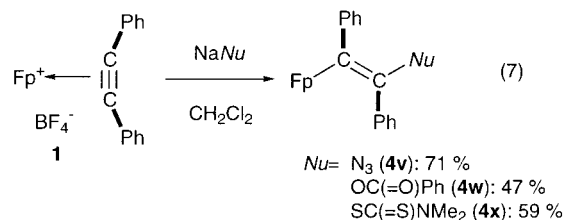


Figure 6. Molecular structures of *trans*-alkenyl complexes **4o**, **4t**, and **13f** drawn at the 30% probability level.



Reaction with inorganic and organic salts (NaN_3 , PhCOONa , $\text{Me}_2\text{NCS}_2\text{Na}$) produced *trans*-alkenyl complexes **4v**, **w**, **x** as sole organometallic products in moderate yields (eq 7),¹³ and their *trans*-configuration has been determined by X-ray crystallography.⁹



Carbon nucleophiles such as silyl enol ether and allylstannane readily reacted with **1** to give adducts **4y** and **7a** (Chart 2),^{13,14} although no reaction was observed with allylsilane ($\text{CH}_2=\text{CHCH}_2\text{SiMe}_3$). Reaction with a bulky phenolate, $\text{NaOC}_6\text{H}_3\text{-2,6-Bu}'_2$, did not result in

(13) Yields shown are isolated yields.

(14) Chromatographic purification gave **4z** as an isomeric mixture with **3z**, but recrystallization of the mixture afforded **3z** as single crystals.

entry	Nu	pK_b^b	yields (%)			
			4	5	Fp_2	total
1	$\text{OC}_6\text{H}_4\text{-OPh-}p$ (l)	-	54 (4l) ^c	0	10	64
2	$\text{OC}_6\text{H}_4\text{-OMe-}p$ (m)	3.79	18 (4m)	23 (5m)	10	51
3	$\text{OC}_6\text{H}_4\text{-Me-}o$ (n)	3.87	0	22 (5n)	9	50 ^d
4	$\text{OC}_6\text{H}_4\text{-Me-}p$ (o)	3.80	22 (4o) ^c	23 (5o)	9	54
5	OC_6H_5 (p)	4.11	58 (4p)	0	8	66
6	$\text{OC}_6\text{H}_4\text{-F-}p$ (q)	4.19	58 (4q) ^c	0	6	64
7	$\text{OC}_6\text{H}_4\text{-NO}_2\text{-}p$ (r)	7.15	88 (4r)	0	4	92
8	OC_6F_5 (s)	8.47	85 (4s) ^c	0	0	85

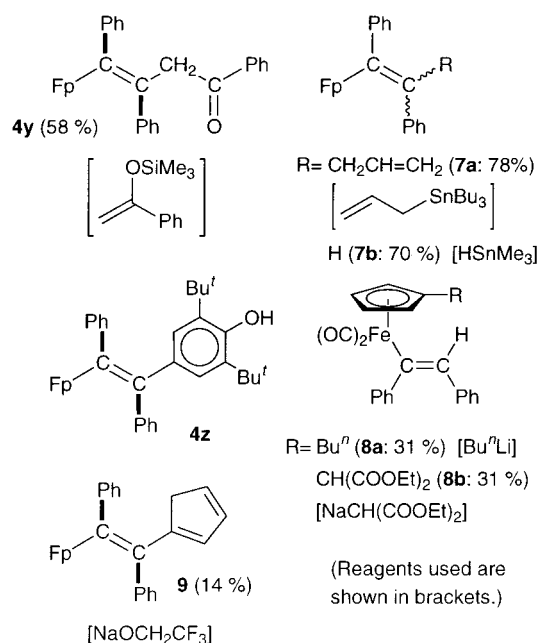
^a determined by $^1\text{H-NMR}$. ^b ref. 8. ^c characterized by X-ray crystallography.

^d Ferrocene (19%) was also formed. ^e NaOC_6F_5 .

$\text{C}=\text{C}$ moiety was *trans*, as indicated by the molecular structure of **4t**, which is shown in Figure 6.

Reaction of $[\text{Fp}^+(\eta^2\text{-Ph-C}\equiv\text{C-Ph})\text{BF}_4^-$ (1**) with Other Nucleophiles.** To further examine the nucleophilic addition reactions to **1**, some more reactions with inorganic and organic salts and carbon nucleophiles were carried out.

Chart 2



O-alkylation but *C*-alkylation at the sterically less congested *p*-position to give **4z**. Because, when left at ambient temperature, **4z** was converted to *cis*-isomer **3z**, characterized crystallographically,⁹ **4z** was assigned to the *trans*-isomer. Attempted addition reaction with another *O*-nucleophile, $\text{NaOCH}_2\text{CF}_3$, resulted in addition of the Cp functional group (**9**) in a low yield, presumably coming from partial decomposition of the Fp fragment. The configuration of **4y** and **9** was determined to be *trans*,^{9,15} whereas that of the oily allyl complex **7a** could not be determined crystallographically.

n-Butyllithium¹⁶ and diethyl sodiomalonate also reacted with **1**, but replacement at the Cp ligand took place to give the 1,2-diphenylethenyl complexes **8a, b**.¹⁷ Hydride addition with HSnMe_3 gave the expected alkenyl complex **7b**. However, again because the products **7b** and **8a** were oily, their configuration could not be determined crystallographically. Complexes **8a, b** should arise from the intramolecular H-transfer in the (*exo*- η^4 - $\text{C}_5\text{H}_5\text{Nu}$) $\text{Fe}(\text{CO})_2(\eta^2\text{-Ph-C}\equiv\text{CPh})$ intermediate formed by addition to the Cp ring from the *exo*-side, and therefore, their configuration was tentatively assigned to the *cis*-structure. Similar hydride transfer was al-

(15) The *trans* configuration of **4x** and **9** was also confirmed by X-ray crystallography, but their structures could not be refined satisfactorily due to the low quality of crystals. Cell parameters for **4x**: monoclinic; $a = 17.569(4)$ Å, $b = 6.857(2)$ Å, $c = 22.30(1)$ Å, $\beta = 108.77(2)^\circ$, $V = 2543(1)$ Å³. **9**: monoclinic; $a = 8.318(3)$ Å, $b = 17.656(3)$ Å, $c = 14.470(3)$ Å, $\beta = 103.15(2)^\circ$, $V = 2069(2)$ Å³.

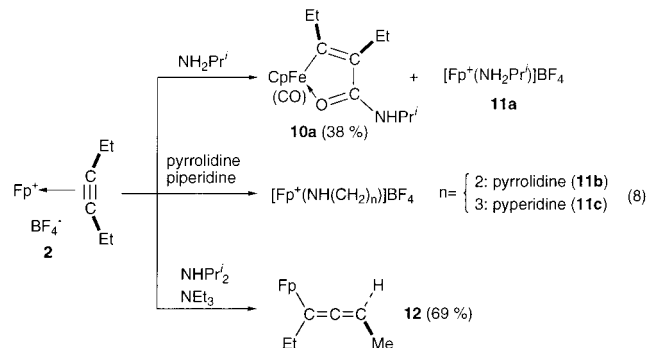
(16) Reaction with *n*-BuLi was carried out in THF.

(17) Spectral data for **8a, b**: **8a**: δ_{H} (CDCl_3) 0.89 (3H, t, CH_3), 1.2–1.7 (4H, m, $(\text{CH}_2)_2$), 2.21 (2H, t, CH_2), 4.57 (2H, m, $\eta^5\text{-C}_5\text{H}_4$), 4.68 (2H, m, $\eta^5\text{-C}_5\text{H}_4$), 6.62–7.55 (11H, m, Ph and =CH); δ_{C} (CDCl_3) 13.8 (q, $J = 123$, CH_3), 22.3, 27.4, 32.7 (t $\times 3$, $J = 125\text{--}128$, CH_2), 85.2, 86.2 (d $\times 2$, $J = 175$, CH in $\eta^5\text{-C}_5\text{H}_4$), 107.1 (s, $\eta^5\text{-C}_5\text{H}_4$), 124.1, 124.6, 125.3, 127.7, 127.9, 128.3, 128.5, 131.6 (d $\times 8$, Ph), 139.2 (d, $J = 153$, =CH), 139.3, 152.4, 156.1 (s $\times 3$, ipso-Ph and =C). **8b**: δ_{H} (CDCl_3) 1.29 (6H, t, CH_3), 4.20 (4H, q, CH_2), 4.76, 5.09 (2H $\times 2$, s $\times 2$, C_5H_4), 6.2–7.8 (11H, m, Ar); δ_{C} (CDCl_3) 13.9 (q, $J = 127$ Hz, CH_2CH_3), 50.6 (d, $J = 133$ Hz, $\text{CH}(\text{COOEt})_2$), 62.2 (t, $J = 151$ Hz, OCH_2), 86.0 (d, $J = 180$ Hz, C_5H_4), 88.1 (d, $J = 183$ Hz, C_5H_4), 94.3 (s, C_5H_4), 124.4, 124.6, 125.3, 127.6, 128.6, 139.1, 150.2 (Ph), 139.8 (d, $J = 154$ Hz, C_β), 155.5 (d, $J = 8$ Hz, C_α), 166.6 (s, C=O), 215.1 (s, CO).

ready reported for the related system, $([\text{CpFe}(\text{CO})(\text{L})-(\eta^2\text{-R-C}\equiv\text{C-R}')]^+ + \text{borohydrides, L} = \text{PPh}_3, \text{P}(\text{OPh})_3; \text{R, R}' = \text{Me, Ph, COOMe})$, by Reger.^{2b}

Reaction of $[\text{Fp}^+(\eta^2\text{-Et-C}\equiv\text{C-Et})\text{BF}_4$ (2**) with Nucleophiles.** Comparative study of the 3-hexyne complex **2** was carried out in order to see the effect of the substituents attached to the acetylene part. As a result, considerably different reactivity was observed as described below.

Reaction with amine resulted in the formation of metallacycle **10**, substituted product **11**, and deprotonated product **12**, depending on the structure of the amine used (eq 8),¹³ and alkenyl complex was not formed at all. Reaction with a less basic primary amine,



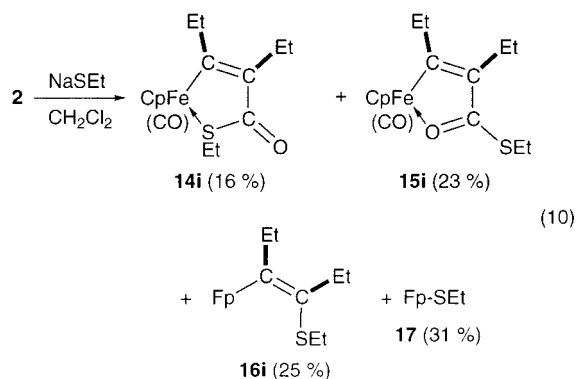
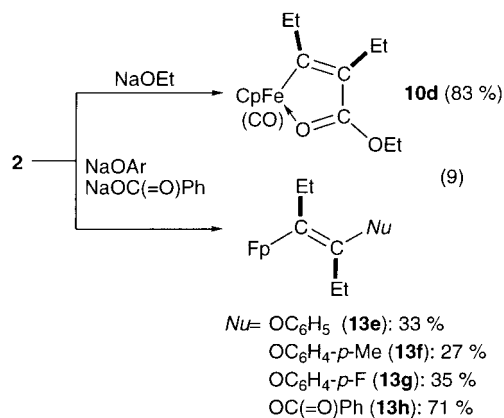
$\text{NH}_2\text{Pr}'$, afforded a mixture of metallacycle **10a** and amine complex **11a**.^{9,18} The former product was readily characterized by comparison with the Ph derivatives **5** [single $\nu(\text{CO})$ and deshielded $\delta_{\text{C}}(\text{C}_\alpha)$]. In the case of the reaction with cyclic secondary amines, $\text{HN}(\text{CH}_2)_n$ ($n = 4, 5$), amine complexes **11b, c**^{9,18} were formed as the sole isolable organometallic products in quantitative yields. Formation of **11** from **2** indicates that the 2-hexyne ligand in **2** is more weakly bound to the iron center than the Ph-C \equiv C-Ph ligand in **1** due to the less effective back-donation to the alkyl-substituted acetylene. In contrast to these reactions, basic amines such as NHPri'_2 and NEt_3 gave oily allenyl complex **12** resulting from deprotonation of a propargyl hydrogen atom. Complex **12** was characterized on the basis of (1) the presence of only one ethyl group, (2) appearance of the methyl signals, and, above all, (3) the three carbon signals assignable to the allenyl part (δ_{C} 76.1, 87.9, 200.3).¹⁹

In the case of the reaction with oxygen nucleophiles, the alkoxide gave metallacycle **10d**, whereas aryloxide and benzoate produced alkenyl complexes **13e–h** (eq 9). The structure of the *p*-methylphenoxy derivative **13f** was confirmed by X-ray crystallography (Figure 6), and the configuration of the benzoate adduct **13h** was tentatively assigned as *trans* on the basis of the configuration of the reaction product of **1** (**4w**).

As a typical example of *S*-nucleophile, reaction with NaSEt was examined (eq 10). Of the four reaction

(18) Amine complexes **11** were characterized by comparison with authentic samples prepared by treatment of $[\text{Fp}(\text{isobutene})]\text{BF}_4$ or $[\text{Fp}(\text{THF})]\text{BF}_4$ with appropriate amines. Molecular structures of **11a, b** were determined by X-ray crystallography. For details, see Supporting Information. The amine complex **11** adopts a typical three-legged piano-stool structure. Some pertinent structural parameters of **11a** are as follows: Fe1–N1 2.015(4) Å; Fe1–C4 1.785(6) Å; Fe–C5 1.780(6) Å; Fe1–C6–10 2.061–2.093(6) Å; N1–Fe1–C4 91.0(2)°; N1–Fe1–C5 93.6(2)°; C4–Fe1–C5 93, 2(3)°. The six substituents attached to the Fe and N atoms adopt a staggered conformation.

(19) Pretsch, P. D.; Seible, J.; Simon, W.; Clerc, T. *Strukturaufklärung Organischer Verbindungen*, 2nd ed.; Springer: Berlin, 1981.

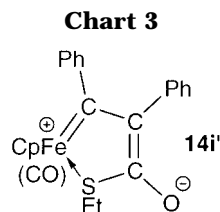


products isolated, two were metallacyclic complexes **14i** and **15i**, which were differentiated by the absence/presence of a $\nu(\text{C}=\text{O})$ vibration as discussed for the **5**- and **6**-type structures of the Ph_2C_2 derivatives, and the former complex **14i** with a $\nu(\text{C}=\text{O})$ absorption (1664 cm^{-1}) was characterized by X-ray crystallography (Figure 4). The structural parameters associated with the cyclic part are essentially the same as those of **5f** as compared in Table 2, indicating the contribution of the zwitterionic carbenic structure **14i'** (Chart 3). The alkenyl complex **16i** could not be isolated in a pure form due to its oily nature, and the *cis*-configuration was tentatively assigned on the basis of the results of the reaction with **1** (**3j,k**) described above. In this case, too, a substantial amount of the substituted product, Fp-SEt ,²⁰ was obtained.

Discussion

Molecular Structures of Cationic η^2 -Alkyne Complexes (1, 2), Alkenyl Complexes (3, 4, 13), and Metallacycles (5, 14). A unit cell of the $\text{Ph-C}\equiv\text{C-Ph}$ complex (**1**) contains two crystallographically independent molecules with essentially the same geometry, but the relative arrangements of the Ph substituents are different. The phenyl rings in molecule **1** are laid essentially coplanar with respect to the Fe1-C101-C102 triangle, whereas those in molecule **2** are laid almost perpendicular to the triangle, as can be seen

(20) Repeated recrystallization of Fp-SEt gave the decarbonylated dimer complex $\text{trans-[CpFe(CO)(}\mu\text{-SEt)]}_2$, **17**, which was characterized crystallographically (Table 4).⁹ Crystal structure of the *cis*-isomer was already reported. Parpiev, N. A.; Toshev, M. T.; Dustov, Kh. B.; Aleksandrov, G. G.; Alekseeva, S. P.; Nekhaev, A. I. *Dokl. Akad. Uzbekskol. SSR* **1988**, 43.



from the side views (Figure 1). In addition, the $-\text{C}\equiv\text{C}-$ linkage in molecule **1** is more twisted with respect to the axis passing through the Fe atom and the midpoint of the $\text{C}\equiv\text{C}$ part. As a result, the C121-126 ring is laid almost coplanar to the Cp ring so that the C102 atom is located closer to the metal center. The $\text{Fe}\cdots\text{C}\equiv$ distances in molecule **1** are slightly shorter than those in molecule **2**. When the structural parameters are compared with the P(OPh)_3 complexes used in Reger's study, $[\text{CpFe}(\text{CO})[\text{P(OPh)}_3](\eta^2\text{-Me-C}\equiv\text{C-R})]\text{-PF}_6$,²¹ no significant and systematic differences are observed within the range of the experimental errors (Table 1). Although the $\text{CpFe}(\text{CO})[\text{P(OPh)}_3]$ fragment is expected to cause elongation of the $\text{C}\equiv\text{C}$ distances and shortening of the $\text{Fe}\cdots\text{C}$ distances due to the more effective back-donation compared to the Fp fragment, the $\text{C}\equiv\text{C}$ distances in **1** [$1.24(2)$, $1.22(1)\text{ \AA}$] and Reger's complexes [$1.19(1)\text{ \AA}$ ($\text{R} = \text{Me}$); $1.21(1)\text{ \AA}$ ($\text{R} = \text{Ph}$)] are comparable and longer than free $\text{Ph-C}\equiv\text{C-Ph}$ [$1.198(3)\text{ \AA}$]²² only by $0.02\text{--}0.04\text{ \AA}$. The slightly longer $\text{C}\equiv\text{C}$ length of the 3-hexyne complex (**2**) [$1.26(2)\text{ \AA}$] may be ascribed to the electron-releasing character of the ethyl substituent compared to the phenyl group in the other complexes. The very similar bent back angles of the alkyne ligands in the four complexes [**1** 22.2° , 27.7° (molecule **1**), 21° , 21° (molecule **2**); **2** 17° , 19° ; $[\text{CpFe}^+(\text{CO})[\text{P(OPh)}_3](\eta^2\text{-Me-C}\equiv\text{C-R})]$ $\text{R} = \text{Me}$, 21.6° , 22.3° ; $\text{R} = \text{Ph}$, 21° , 25°]²¹ are similar to those of $\text{Pt(II)-}\eta^2\text{-alkyne}$ complexes [15° , 18° , $(\eta^2\text{-Bu}^t\text{-C}\equiv\text{C-Bu}^t)\text{PtCl}_2(\text{H}_2\text{-NPh})$;^{23a} 12.7° , 14.5° , $(\eta^2\text{-Ph-C}\equiv\text{C-Ph})\text{Pt}(\text{C}_6\text{F}_5)_2$]^{23b} but are substantially smaller than those in other η^2 -alkyne complexes [$>30^\circ$;²⁴ cf. isoelectronic Cr(0) compound, $(\eta^6\text{-C}_6\text{Me}_6)\text{Cr}(\text{CO})_2(\eta^2\text{-Ph-C}\equiv\text{C-Ph})$, 29.7° , 30.9°].^{24b} These results indicate that back-donation to the η^2 -alkyne ligands in **1** and **2** is not so effective.

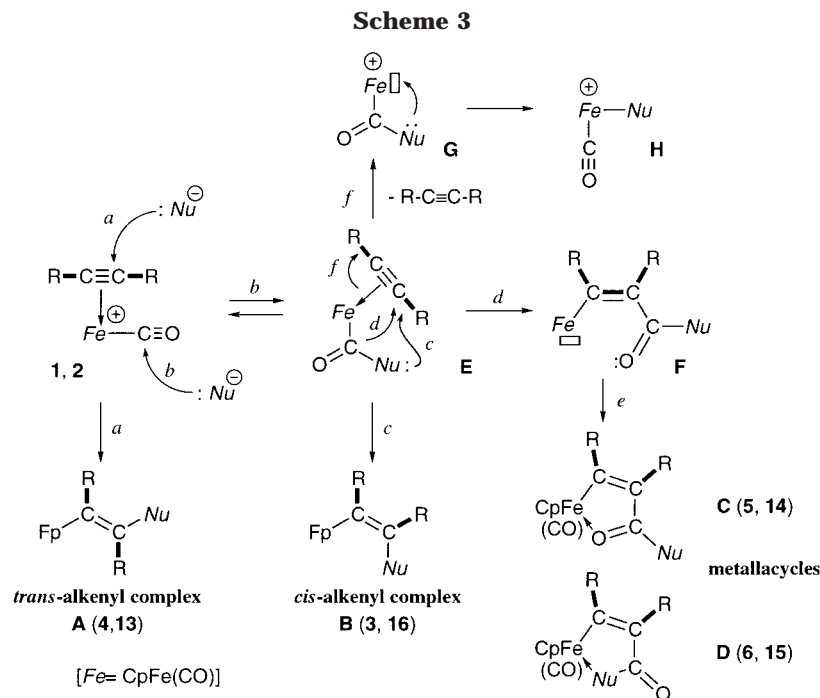
Thus replacement of the P(OPh)_3 ligand by CO does not cause significant change in the structure of the cationic η^2 -alkyne iron complexes, and the small structural deformation of the alkyne ligands in these complexes from free alkyne indicates the rather weak interaction with the metal center in the $[\text{CpFe}(\text{CO})(\text{L})\text{-(}\eta^2\text{-alkyne)}]^+$ -type cationic alkyne complexes. In accord with this consideration, products resulting from alkyne ligand dissociation are occasionally formed as described above.

(21) Reger, D. L.; Klaeren, S. A.; Lebioda, L. *Organometallics* **1988**, 7, 189.

(22) Mavridis, A.; Moustakali-Mavridis, I. *Acta Crystallogr. Sect. B* **1977**, B33, 3612.

(23) (a) Davies, G. R.; Hewertson, D. W.; Mais, R. H. B.; Owston, P. G. *J. Chem. Soc. (A)* **1970**, 1873. (b) Usón, R.; Forníés, J.; Tomás, M.; Menjón, B.; Fortño, C.; Welch, A. J.; Smith, D. E. *J. Chem. Soc., Dalton Trans.* **1993**, 275.

(24) (a) Cappelle, B.; Dartiguenave, M.; Dartiguenave, Y.; Beauchamp, A. L. *J. Am. Chem. Soc.* **1983**, 105, 4662. (b) Bartlett, I. M.; Connelly, N. G.; Orpen, A. G.; Quayle, M. J.; Rankin, J. C. *J. Chem. Soc., Chem. Commun.* **1996**, 2583. Davies, G.; Hewertson, W.; Mais, R. H. B.; Owston, P. G.; Patel, C. G. *J. Chem. Soc. (A)* **1970**, 1873. Usón, R.; Forníés, J.; Tomás, M.; Menjón, B.; Fortnup, C. *J. Chem. Soc., Dalton Trans.* **1993**, 275.



In accord with the discussion on the solid-state structure, the ^{13}C NMR signals of the alkyne carbon atoms are observed around 50 ppm [δ_{C} 58.0 (**1**), 50.3 (**2**); $[\text{CpFe}^+(\text{CO})[\text{P}(\text{OPh})_3](\eta^2\text{-Me-C}\equiv\text{C-R})]$ 46.4 (R = Me), 51.5, 57.8 (R = Ph)] upfield compared with that of free $\text{Ph-C}\equiv\text{C-Ph}$ [δ_{C} 89.5].¹⁰

Alkenyl complexes **3**, **4**, and **13** adopt typical three-legged piano-stool structures. No significant and systematic change of the structural parameters depending on the *Nu* part (Table 2) can be observed. Although we also attempted spectroscopic determination of the configuration of the alkenyl moiety,^{2c} no systematic difference between the *cis*- and *trans*-isomers was observed.²⁵

Structural features of metallacycles **5** and **14** can be rationalized in terms of contribution of the carbenic structures such as **5'** and **14i'** as discussed above. While the ^1H and ^{13}C NMR signals of the Cp ligand in metallacycles appear in slightly lower field compared to those of alkenyl complexes (Table S1 and S2), they were readily differentiated by the number of ν_{CO} absorptions [1 (metallacycle) vs 2 (alkenyl complexes)] as discussed above.

Reaction Mechanisms. Reaction of the cationic iron η^2 -alkyne complexes **1** and **2** affords various products including alkenyl complexes [**A** (*trans*), **4**, **13**; **B** (*cis*), **3**, **16**] and metallacyclic compounds [**C**, **5**, **14**; **D**, **6**, **15**]. The formation of these products from anionic nucleophiles such as alkoxide, aryloxy, and alkane- and arenethiolate is explained in terms of the mechanism summarized in Scheme 3. Direct nucleophilic addition to the alkyne carbon atom from the side opposite the metal center with respect to the $\text{C}\equiv\text{C}$ part furnishes *trans*-alkenyl complexes **A** (path *a*). The “*trans*-addition rule” has been explained by this mechanism. On the other hand, initial nucleophilic addition to the carbonyl ligand would give rise to the acyl intermediate **E** (path

b),¹ from which two pathways are feasible. The nucleophile part in **E** still has lone pair electrons, which may attack the alkyne carbon atom from the inner side to give the *cis*-alkenyl complexes **B** (path *c*).²⁶ Migration of the whole acyl group would give the coordinatively unsaturated species **F**, and subsequent coordination of either the acyl oxygen atom or the nucleophile part (path *e*) furnishes the metallacyclic products, **C** or **D**, respectively. A third mechanism operates in some cases. Dissociation of the $\text{Ph-C}\equiv\text{C-Ph}$ ligand from **E** (path *f*) followed by retromigratory insertion of the nucleophile part leads to the formation of Fp-Nu **H**, which may be further converted to Fp_2 via Fe-Nu homolysis or β -hydride elimination. Fp_2 may be also formed by direct electron transfer from the nucleophile to the cationic η^2 -alkyne complex (**1** and **2**). Elimination of the η^2 -alkyne ligand from the resulting **19e** species releases the **17e** radical species (Fp^\bullet),²⁷ dimerization of which leads to Fp_2 .

Many precedents have been reported for the formation of the metallacyclic product via an $(\eta^1\text{-acyl})(\eta^2\text{-alkyne})$ intermediate like **E** (path *d*). Such a species can be alternatively generated by CO insertion of an (alkyl)-(carbonyl) complex induced by coordination of an alkyne ligand or nucleophilic addition to a metal carbonyl complex in the presence of alkyne, as we reported previously.^{6c,28} In contrast to this pathway, path *c* leading to the *cis*-alkenyl complex has few precedents. Acyl group migration giving **F** (path *d*) may be interpreted in terms of a metathesis-like mechanism, when the contribution of the oxycarbene structure [$\text{M}^+=\text{C}(\text{O}^-)\text{-R}$] for the acyl species is taken into account.

In the case of the reaction with amines, formation of products involves nucleophilic addition as well as de-

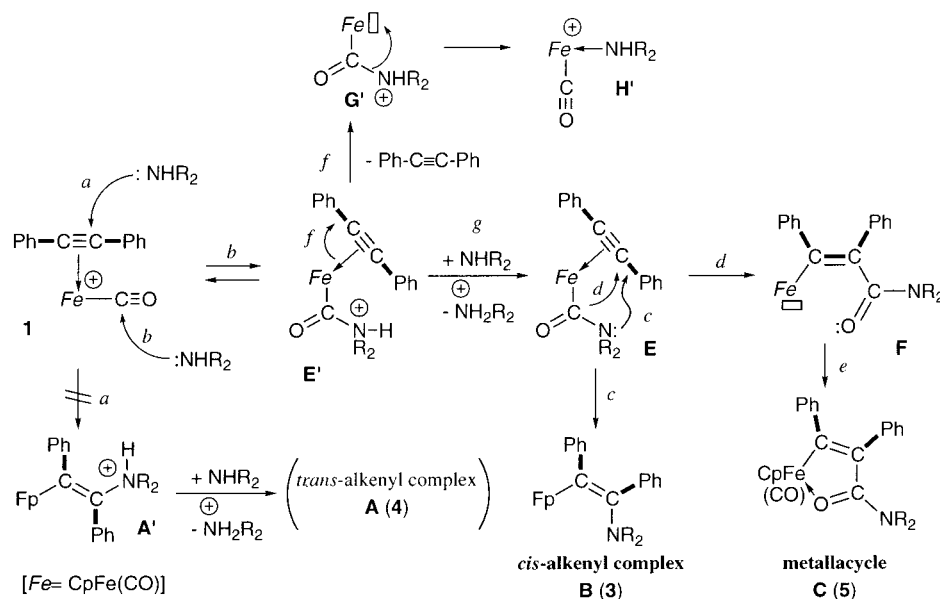
(25) In some cases ^{13}C NMR signals for the olefinic carbon atoms could be assigned by careful examination of the coupling pattern, but definite assignments were not always possible due to similar appearance of the *ipso*-carbon signals of the phenyl rings.

(26) The acetyl analogue of **E**, $\text{CpFe}(\text{CO})(\text{Ph-C}\equiv\text{C-Ph})\text{-C(=O)-Me}$, which has no lone pair electrons at the position corresponding to *Nu*, can be generated by a different method.^{6c} In this case, metallacycle was formed exclusively due to the lack of lone pair electrons.

(27) Astruc, D. *Chem. Rev.* **1988**, *88*, 1189. Baird, M. C. *Chem. Rev.* **1988**, *88*, 1217.

(28) Templeton, J. L. *Adv. Organomet. Chem.* **1989**, *29*, 1.

Scheme 4



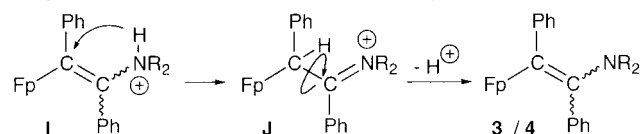
protonation, and we propose the modified mechanism shown in Scheme 4.²⁹ Because no *trans*-alkenyl complex **4** is obtained, the reaction does not follow path *a* but path *b*, which involves initial attack of amine at the CO ligand to give the ammonium intermediate **E'** (path *b*).

Formation of the *cis*-alkenyl complex **B** should be preceded by deprotonation (path *g*), because no lone pair electrons are present on the nitrogen atom in the ammonium intermediate **E'**. On the resulting acyl intermediate **E**, the process analogous to Scheme 3 should lead to *cis*-alkenyl complexes **B**(**3**) and metallacycles **C**(**5**) via the deprotonation–migration sequence.

Factors Determining the Regiochemistry of Nucleophilic Addition. Taking into account the product distribution and the reaction mechanisms, factors determining the regiochemistry of the nucleophilic addition are considered.

The clear-cut dependence of the product distribution on the substituents of nucleophiles (alkyl vs aryl) suggests that basicity (nucleophilicity) of the nucleophile may affect the reaction pathway. To consider the initial nucleophilic addition sites, the distribution of three types of olefinic products, *trans*-alkenyl complex (**A**), *cis*-alkenyl complex (**B**), and metallacycles (**C** and **D**), is

(29) The result of the reaction with Bu⁺NH₂, which afforded a different type of product, **3c'** (eq 2), arouses suspicion that stereochemistry of the alkenyl products **3** and **4** may not be retained in the reaction system. The **3c'**-type product **J** should be formed by H-migration of the initially formed ammonioalkenyl intermediate **I**. C–C rotation followed by deprotonation would cause stereochemical scrambling of the alkenyl moiety. At least the reaction with primary amine (NR₂ = NHalkyl) does not follow such a reaction pathway, as revealed by the deprotonation experiment (eq 3). Although the possibility cannot be completely excluded for the reactions with secondary amines, we inferred, from (1) formation of a single isomer of alkenyl complex (**3/4**), (2) *cis*-stereochemistry observed for the reaction with NaSR, and (3) the uniform dependence of the product distribution on p*K*_B values of nucleophiles (see below), that the H-induced stereochemical scrambling was not viable in the present reaction system.



summarized according to the p*K*_B value of the nucleophiles (Figure 7).^{8,30} Fp₂ is eliminated from the distribution, because it can be formed via various mechanisms as discussed above. Let us note that products **B**, **C**, and **D** arise from the initial nucleophilic addition to the CO ligand (path *b* in Schemes 3 and 4) and that *exo*-attack to the alkyne ligand leads to **A** (path *a*). Taking into account this point, we can see a dramatic change in the distribution around the p*K*_B value of 4. In other words, the reaction site switches depending on the basicity of nucleophiles. Nucleophiles with a small p*K*_B value (a basic nucleophile) attack the carbonyl ligand to give the olefinic products with the *cis*-Ph–C=C–Ph linkage (**B**, **C**, and **D**), whereas nucleophiles with a larger p*K*_B value (a less basic nucleophile) attack the alkyne ligand from the *exo*-side to give *trans*-alkenyl complex **A**.

The key point of this interpretation is competition between the nucleophilic addition to the alkyne carbon atom (path *a*) and CO (path *b*) (Schemes 3 and 4).³¹ The former step (path *a*) is an irreversible one, and reversibility of the latter process (path *b*) depends on the basicity of nucleophiles. In the case of the reaction with a stronger base the equilibrium of path *b* should be shifted to the side of **E**, because formation of a neutral species **E** is favored over the separation of highly charged species: the cationic Fe–alkyne complexes (**1**, **2**) and the anionic nucleophile. In this case, the reaction may proceed virtually in an irreversible manner to give **B**, **C**, and **D** with the *cis*-Ph–C=C–Ph linkage. On the other hand, the equilibrium for a weak base is not completely shifted to the side of acyl intermediate **E**, and back reaction regenerating the starting complex may be feasible. In the meantime, the irreversible *exo*-attack (path *a*) would lead to the formation of *trans*-alkenyl complex **A**.

(30) The result of NaOC₆H₄–Me-*o* (**n**) was removed for clarity, because small changes in the p*K*_B value around 4 (differences between **m** and **o** < 0.07) might cause a drastic change in the product distribution. The removal did not cause any significant change of the conclusion.

(31) Liu, L.-K.; Eke, U. B.; Mesubi, M. A. *Organometallics* **1995**, *14*, 3958.

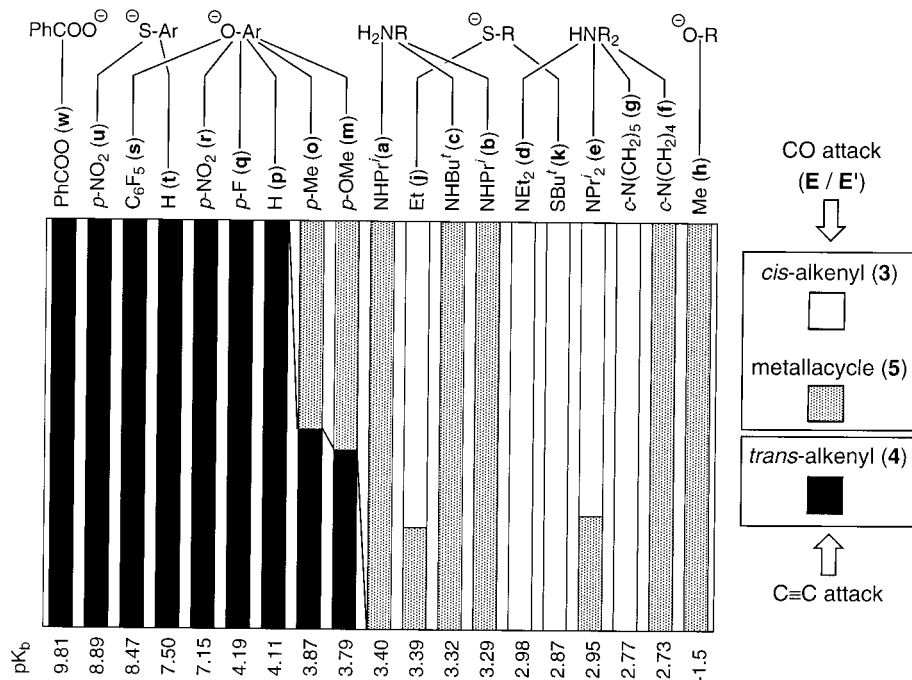
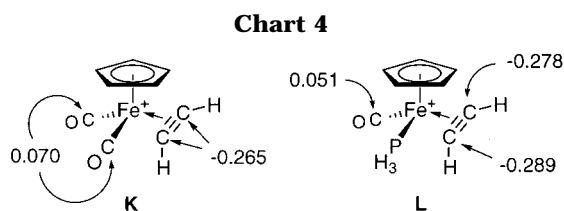
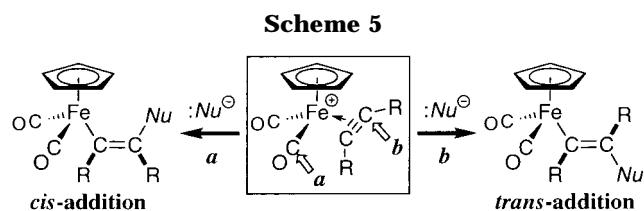


Figure 7. Dependence of the product distribution of the nucleophilic addition reactions to **1** on pK_b values of nucleophiles.



As for the selectivity between *cis*-alkenyl complex **B** and metallacycle **C/D**, the result of the reaction with amine (eq 1) suggests that steric bulkiness of the nucleophile has some influence on the reaction pathways, but any decisive conclusion cannot be deduced from the results obtained so far.

Thus two initial nucleophilic addition sites are feasible for **1** and **2**. This result is in sharp contrast to Reger's system, where addition to CO was not observed at all and only *trans*-additions were obtained. To see the electronic state of the ligands attached to the iron center in these systems, the electron density is calculated for the simplified model complexes, $[\text{Fp}^+(\eta^2\text{-H-C}\equiv\text{C-H})]$ (**K**) and $[\text{CpFe}^+(\text{CO})(\text{PH}_3)(\eta^2\text{-H-C}\equiv\text{C-H})]$ (**L**), by EHMO (Chart 4).³² In the former species, the CO ligands are the only positively charged sites, and the alkyne carbon atoms are negatively charged. This result is consistent with the preferred addition to CO as observed for the Fp complexes **1** and **2**. Introduction of the PH_3 ligand (**L**) causes increase of the electron density at both the alkyne and CO moieties. The CO ligand is still the only positively charged site in the molecule, and the alkyne carbon atoms are more negatively charged than those in the Fp complexes. The increase of the negative charge at CO, however, should hinder the nucleophilic addition to the CO ligand so as to drive the reaction to path *a* (Scheme 3).³³ The *trans*-addition observed for Reger's system, therefore, may be ascribed to the shift of the CO addition equilibrium as well as the steric shielding of the CO ligand by the bulky PR_3 ligand. As a result of



the electronic and steric effects, the nucleophile should attack the alkyne ligand from the *exo*-side to give *trans*-alkenyl complexes.³⁴

Conclusion

The present study has revealed that (1) *trans*-addition is not always the unique stereochemical outcome upon nucleophilic addition to transition metal η^2 -alkyne complexes bearing a π -acid such as CO and (2) stereochemistry (product distribution) is dependent on the reaction site (*a* vs *b*), which is governed by basicity (nucleophilicity) of nucleophiles (Scheme 5). Because, in many cases, carbonyl ligands are involved as auxiliary ligands of alkyne complexes, the stereochemistry of alkenyl complexes obtained by nucleophilic addition to η^2 -alkyne complexes should be examined carefully by means of crystallography combined with various spectroscopic techniques. Inadvertent application of the "*trans*-addition rule" leads to misinterpretation of the stereochemistry of nucleophilic addition.

Experimental Section

General Considerations. All manipulations were carried out under an inert atmosphere by using standard Schlenk tube

(33) We are grateful to the reviewer's comment on the consideration of the electronic effect. The reviewer also suggested to examine the addition rates of strong and weak nucleophiles. We attempted kinetic measurements of the nucleophilic addition at low temperatures, but the reactions were too fast to be followed by NMR. No apparent difference could be detected.

(34) Slippage of the alkyne ligand induced by the unsymmetrical electronic structure of the PR_3 -substituted complexes may be another possible reason for the *trans*-addition. Eisenstein, O.; Hoffmann, R. J. *Am. Chem. Soc.* **1981**, *104*, 4308.

(32) *CACHE 4.0*, Oxford Molecular, 1997.

techniques. Ether, hexanes (Na–K alloy), and CH_2Cl_2 (P_2O_5) were treated with appropriate drying agents, distilled, and stored under argon. The cationic iron η^2 -alkyne complexes **1** and **2** were prepared from the isobutene complex $[\text{Fp}^+(\eta^2\text{-CH}_2=\text{CMe}_2)]\text{BF}_4$,³⁵ following the reported method.⁷ Sodium alkoxides were prepared by careful addition of small pieces of Na metal to a large amount of alcohol, and the volatiles were removed from the resulting solution to give a colorless solid, which was used without further purification. Sodium salts of phenol and arenethiol derivatives were synthesized by treatment of appropriate phenol or arenethiol with NaH (~0.8 equiv) suspended in ether followed by filtration, washing with ether, and drying under reduced pressure. Other chemicals were purchased and used as received. Chromatography was performed on alumina [aluminum oxide, activity II–IV (Merck Art. 1097)]. ^1H and ^{13}C NMR spectra were recorded on JEOL EX-400 (^1H , 400 MHz; ^{13}C , 100 MHz) and JEOL EX-90 spectrometers (^1H , 90 MHz). Multiplicity, coupling constants ($J_{\text{C-H}}$ in Hz), and assignments are shown in parentheses. Solvents for NMR measurements containing 0.5% TMS were dried over molecular sieves, degassed, distilled under reduced pressure, and stored under Ar. IR spectra were obtained on a JASCO FT/IR 5300 spectrometer.

Spectroscopic and analytical data for new compounds not shown below are summarized in Tables S1–S3 (Supporting Information). Of more than 40 new compounds reported in this paper, satisfactory results of elemental analysis were not obtained for oily products, **3z**, **6j**, **8**, **14i**, and **15i**.

Reaction of $[\text{Fp}^+(\eta^2\text{-R-C}\equiv\text{C-R})]\text{BF}_4$ (1** and **2**) with Nucleophiles.** The reaction was carried out in CH_2Cl_2 . The product distribution was determined by ^1H NMR experiments. A typical procedure was as follows. To a stirred CH_2Cl_2 solution of **1** cooled at -78°C was added nucleophile (> 5 equiv), and then the mixture was gradually warmed to room temperature. After the completion of the reaction was checked by TLC (disappearance of the orange spot of **1** at the origin), the volatiles were removed under reduced pressure. The products were extracted with CH_2Cl_2 , and the insoluble materials were removed by filtration through an alumina plug. After the volatiles were removed under reduced pressure, CDCl_3 (0.4 mL) and an internal standard (anisole) was added to the residue, and the product distribution was determined by comparison of intensities of the Cp signals and the MeO signal of anisole.

In some cases, reaction was carried out in CD_2Cl_2 , and the product distribution was determined by ^1H NMR after addition of an internal standard (anisole).

Several typical experimental procedures for isolation of products are described below in detail.

Reaction of **1 with NHPr^i_2 .** To a CH_2Cl_2 solution (10 mL) of **1** (223 mg, 0.51 mmol) cooled at -78°C was added NHPr^i_2 (0.5 mL) slowly. Then the cooling bath was removed, and the mixture was gradually warmed to ambient temperature. During this period, the solution color changed from orange to yellow green. After the mixture was stirred for 1 h, the completion of the reaction was checked by TLC (disappearance of the orange spot at the origin), and then the volatiles were removed under reduced pressure. The residue was extracted with hexanes and passed through an alumina plug. Crystallization from Et_2O –hexanes gave **3e** (168 mg, 0.37 mmol, 72% yield) as yellow orange crystals. Anal. Calcd for $\text{C}_{27}\text{H}_{29}\text{NO}_2\text{Fe}$: C, 71.21; H, 6.42; N, 3.08. Found: C, 71.27; H, 6.46; N, 3.10.

Reaction of **1 with Bu^tNH_2 .** To a CH_2Cl_2 solution (27 mL) of **1** (554 mg, 1.25 mmol) cooled at -78°C was added Bu^tNH_2 (1.58 mL, 15.0 mmol). Then the cooling bath was removed, and the mixture was gradually warmed to ambient temperature. After the mixture was stirred for 1 h, the volatiles were

removed under reduced pressure. The residue was extracted with CH_2Cl_2 and passed through an alumina plug. Addition of hexanes and cooling at -30°C afforded a solid containing $[\text{Fp}(\text{Bu}^t\text{NH}_2)]\text{BF}_4$. Further concentration of the supernatant solution followed by addition of ether and cooling gave **3c'** (155 mg, 0.30 mmol, 24% yield) as brick red crystals. Chromatographic separation of the supernatant solution gave **5c** (brown band, 53 mg, 0.12 mmol, 10% yield) and Fp_2 (red-brown band). **3c'**: δ_{H} (CDCl_3) 1.24 (9H, s, Bu^t), 4.89 (5H, s, Cp), 5.35 (1H, br, Fe–CH), 6.80–7.52 (10H, m, Ph), 10.20 (1H, br, NH); δ_{C} (CDCl_3) 30.9 (q, 128, CMe_3), 31.1 (d, 128, C_ω), 60.9 (s, CMe_3), 88.5 (d, 183, Cp), 125.5, 127.8, 128.0, 128.1, 129.2, 130.8, 131.1, 141.7 (Ph signals), 198.9 (s, C=N), 215.0, 215.6 (s \times 2, CO). IR (KBr): ν_{NH} 3261, ν_{CO} 2021, 1967, ν_{BF} 1084 cm^{-1} . Anal. Calcd for $\text{C}_{25.5}\text{H}_{27}\text{O}_2\text{NCIBF}_4\text{Fe}$ [**3c'**·(CH_2Cl_2)_{1/2}]: C, 54.94; H, 4.84; N, 2.51. Found: C, 54.95; H, 5.05; N, 2.60.

Treatment of **3c' with NEt_3 .** To complex **3c'** (670 mg, 1.30 mmol) dissolved in CH_2Cl_2 (1.5 mL) was added NEt_3 (0.24 mL, 1.69 mmol) with stirring. Addition of hexane and ether caused precipitation of inorganic salts and Fp_2 . The supernatant solution was passed through a Celite plug, and the volatiles were removed under reduced pressure. The residue was subjected to column chromatography and eluted with CH_2Cl_2 /hexane = 1:3. The deep yellow band was collected, and **3c''** (129 mg, 0.30 mmol, 18% yield) was obtained as a yellow solid after evaporation. Because **3c''** was not so stable, it was subjected to spectroscopic analysis after extraction with ether, filtration through an alumina plug, and evaporation. Because repeated crystallization caused decomposition of **3c''** to give organic products [$\text{PhCH}_2\text{C}(=\text{O})\text{Ph}$ and $\text{PhC}(=\text{O})\text{NHBu}^t$], an analytically pure sample of **3c''** could not be obtained.

Reaction of **1 with NaOMe.** To a CH_2Cl_2 solution (25 mL) of **1** (1.12 g, 2.53 mmol) cooled at -78°C was added THF (60 mL) and then NaOMe (0.89 g, 16.5 mmol) with stirring. After 3 min the cooling bath was removed, and the resultant mixture was stirred for 1 h at ambient temperature. The mixture changed from orange to dark red and then black. After removal of the volatiles, products were separated by column chromatography and then preparative TLC. From dark brown and yellow bands **5h** (0.37 g, 0.79 mmol, 31% yield)^{6c} and **5h'** (100 mg, 0.38 mmol, 15% yield) were obtained, respectively. **5h'**: δ_{H} (CDCl_3) 3.81 (3H, s, OMe), 7.40, 7.42–7.57 (9H, m, aromatic). δ_{C} (CDCl_3) 52.1 (q, 148, OMe), 122.7 (dd, 166, 7), 123.8 (dd, 164, 7), 128.0 (dd, 158, 7), 129.1 (dt, 164, 7), 129.2 (dt, 164, 7), 129.7 (dt, 167, 6), 133.8 (d, 7), 135.3 (d, 7), 138.6 (s); aromatic carbon atoms, 165.0 (s, C=O), 195.0 (s, COOMe). IR (KBr): $\nu_{\text{C=O}}$ 1717 cm^{-1} . Anal. Calcd for $\text{C}_{17}\text{H}_{12}\text{O}_3$: C, 77.29; H, 4.54. Found: C, 77.05; H, 4.52.

Reaction of **1 with NaSBu^t .** To a THF solution (20 mL) of NaSBu^t (1.04 g, 8.9 mmol) cooled at -78°C was added dropwise **1** (1.56 mg, 3.53 mmol) dissolved in THF (30 mL). Then the cooling bath was removed, and the mixture was gradually warmed to ambient temperature. During this period, the solution color changed from orange to yellow green. After the mixture was stirred for 1 h, the volatiles were removed under reduced pressure. The residue was extracted with ether and passed through an alumina plug to remove salts. Chromatographic separation (CH_2Cl_2 /hexanes = 1:10 to 1:7) gave three organometallic products in the order **3k**, **4k**, and **6k**. Crystallization from hexanes gave orange **3k** (185 mg, 0.42 mmol, 12% yield), yellow **4k** (134 mg, 0.30 mmol, 9% yield), and orange **6k** (104 mg, 0.23 mmol, 7% yield) as microcrystals. Anal. **3k**: Calcd for $\text{C}_{25}\text{H}_{24}\text{O}_2\text{SFe}$: C, 67.57; H, 5.44. Found: C, 67.28; H, 5.34. **4k**: Calcd for $\text{C}_{25}\text{H}_{24}\text{O}_2\text{SFe}$: C, 67.57; H, 5.44. Found: C, 67.15; H, 5.34. **6k**: Calcd for $\text{C}_{25}\text{H}_{24}\text{O}_2\text{SFe}$: C, 67.57; H, 5.44. Found: C, 67.15; H, 5.34.

Reaction of **1 with $\text{NaOC}_6\text{H}_4\text{-}p\text{-F}$.** To a CH_2Cl_2 solution (10 mL) of **1** (223 mg, 0.51 mmol) cooled at -78°C was added $\text{NaOC}_6\text{H}_4\text{-}p\text{-F}$ (234 mg, 1.74 mmol) as a solid in one portion. Then the cooling bath was removed, and the mixture was gradually warmed to ambient temperature. After the mixture

(35) Rosenblum, M.; Giering, W. P.; Samuels, A.-B. *Inorg. Synth.* **1990**, *28*, 207.

Table 4. Crystallographic Data

	1	2	3e	3c' (CH ₂ Cl ₂) _{1/2}	5c	5f	5h'	3k
formula	C ₂₁ H ₁₅ O ₂ FeBF ₄	C ₁₃ H ₁₅ O ₂ FeBF ₄	C ₂₇ H ₂₉ NO ₂ Fe	C _{25.5} H ₂₇ NO ₂ Fe-BF ₄ Cl	C ₂₅ H ₂₅ NO ₂ Fe	C ₂₅ H ₂₃ NO ₂ Fe	C ₁₇ H ₁₂ O ₃	C ₂₅ H ₂₄ O ₂ FeS
fw	442.0	345.9	455.4	557.6	427.3	425.3	264.3	444.4
cryst syst	triclinic	monoclinic	monoclinic	monoclinic	monoclinic	monoclinic	monoclinic	monoclinic
space group	<i>P</i> $\bar{1}$	<i>C2/c</i>	<i>P2₁/n</i>	<i>P2/a</i>	<i>P2/c</i>	<i>P2₁/a</i>	<i>P2₁/n</i>	<i>P2₁/a</i>
<i>a</i> /Å	14.144(6)	16.925(6)	13.951(5)	28.35(2)	9.716(2)	12.034(3)	8.671(2)	9.193(4)
<i>b</i> /Å	14.570(7)	14.213(4)	17.314(8)	10.031(7)	18.969(4)	18.66(1)	18.058(3)	33.201(8)
<i>c</i> /Å	10.129(2)	14.211(5)	10.245(2)	9.619(5)	12.645(2)	9.776(5)	8.723(3)	8.272(3)
α /deg	102.95(2)							
β /deg	99.65(3)	111.44(2)	105.62(8)	99.45(5)	109.14(1)	110.0(1)	108.86(2)	115.12(8)
γ /deg	103.38(4)							
<i>V</i> /Å ³	1925(2)	3182(2)	2383(3)	2698(3)	2201.7(7)	2063(3)	1292.5(6)	2286(2)
<i>Z</i>	4	8	4	4	4	4	4	4
<i>d</i> _{calc} /g·cm ⁻³	1.53	1.44	1.27	1.37	1.29	1.37	1.36	1.29
μ /cm ⁻¹	8.3	9.9	6.5	7.07	7.04	7.5	0.93	7.67
2 θ /deg	2–53	5–50	2–50	5–50	5–50	2–55	5–55	2–55
diffractometer	AFC5S	AFC5R	AFC5S	AFC7R	AFC7R	AFC5S	AFC7R	AFC5R
no. of data collected	8450	3027	4591	5409	4268	5195	3265	5707
no. of data with <i>I</i> > 3 σ (<i>I</i>)	4479	1631	2210	2716	2366	1850	1904	2793
no. of variables	489	175	280	333	262	262	229	261
isotropic refinement	B2, F5–8	B1,2, F1–8		H1,2				
<i>R</i>	0.079	0.085	0.080	0.064	0.047	0.057	0.041	0.072
<i>R</i> _w	0.076	0.080	0.065	0.057	0.033	0.042	0.029	0.057

	4l	4o	4q	4s	4t	4v	4w	4y
formula	C ₃₃ H ₂₄ O ₄ Fe	C ₂₈ H ₂₂ O ₃ Fe	C ₂₇ H ₁₉ FO ₃ Fe	C ₂₇ H ₁₅ F ₅ O ₃ Fe	C ₂₇ H ₂₀ SO ₂ Fe	C ₂₁ H ₁₅ N ₃ O ₂ Fe	C ₂₈ H ₂₀ O ₄ Fe	C ₂₉ H ₂₂ O ₃ Fe
fw	540.4	462.3	466.3	538.3	464.4	397.2	476.3	474.3
cryst syst	monoclinic	orthorhombic	orthorhombic	triclinic	orthorhombic	monoclinic	orthorhombic	orthorhombic
space group	<i>C2/c</i>	<i>P2₁2₁2₁</i>	<i>P2₁2₁2₁</i>	<i>P</i> $\bar{1}$	<i>P2₁2₁2₁</i>	<i>P2₁</i>	<i>Pna2₁</i>	<i>P2₁2₁2₁</i>
<i>a</i> /Å	24.277(5)	18.989(6)	18.184(3)	9.685(3)	17.376(5)	8.599(1)	17.147(4)	6.406(5)
<i>b</i> /Å	11.692(3)	6.479(5)	18.405(2)	13.464(4)	19.83(1)	13.703(4)	6.546(4)	17.524(5)
<i>c</i> /Å	18.988(4)	17.919(5)	6.494(2)	9.080(3)	6.508(2)	7.711(2)	20.221(3)	20.332(6)
α /deg				101.91(3)				
β /deg	101.70(1)			98.79(3)		95.10(2)		
γ /deg				91.91(2)				
<i>V</i> /Å ³	5279(2)	2205(3)	2173.3(7)	1142.3(6)	2243(1)	905.0(6)	2270(2)	2283(1)
<i>Z</i>	8	4	4	2	4	2	4	4
<i>d</i> _{calc} /g·cm ⁻³	1.36	1.39	1.43	1.57	1.38	1.46	1.39	1.38
μ /cm ⁻¹	6.0	7.1	7.2	7.2	7.8	8.5	7.0	6.9
2 θ /deg	5–50	5–55	5–60	5–50	5–50	2–50	5–60	5–55
diffractometer	AFC5R	AFC5R	AFC5R	AFC5R	AFC5R	AFC5S	AFC5R	AFC5R
no. of data collected	5005	5668	3571	5556	2951	1801	3888	3136
no. of data with <i>I</i> > 3 σ (<i>I</i>)	2583	1760	2556	3985	1571	1498	2648	1108
no. of variables	343	239	289	325	280	243	298	133
isotropic refinement		C12–26						C8–38
<i>R</i>	0.040	0.059	0.038	0.041	0.060	0.036	0.035	0.088
<i>R</i> _w	0.031	0.056	0.026	0.035	0.034	0.025	0.022	0.060

	3z	11a	11c	13f	14i	17
formula	C ₃₅ H ₃₆ O ₃ Fe	C ₁₀ H ₁₄ NO ₂ FeBF ₄	C ₃₉ H ₃₁ NO ₂ FeB	C ₂₀ H ₂₂ O ₃ Fe	C ₁₅ H ₂₀ O ₂ SFe	C ₁₆ H ₂₀ O ₂ S ₂ Fe ₂
fw	560.5	322.9	612.3	366.2	320.2	420.2
cryst syst	triclinic	orthorhombic	orthorhombic	orthorhombic	orthorhombic	monoclinic
space group	<i>P</i> $\bar{1}$	<i>Pbca</i>	<i>Pna2₁</i>	<i>Pbca</i>	<i>Pbca</i>	<i>P2₁/c</i>
<i>a</i> /Å	10.390(2)	14.652(4)	20.802(4)	19.59(1)	16.026(3)	7.759(3)
<i>b</i> /Å	16.641(3)	14.637(2)	9.852(2)	21.432(8)	33.059(6)	12.272(3)
<i>c</i> /Å	9.366(1)	12.755(2)	14.831(3)	8.840(6)	5.970(3)	9.765(2)
α /deg	106.04(1)					
β /deg	95.68(1)					109.60(2)
γ /deg	74.65(2)					
<i>V</i> /Å ³	1500.1(5)	2735(1)	3039(2)	3712(4)	3163(2)	875.9(4)
<i>Z</i>	2	8	4	8	8	2
<i>d</i> _{calc} /g·cm ⁻³	1.24	1.57	1.34	1.31	1.35	1.59
μ /cm ⁻¹	5.3	11.4	5.32	8.2	10.7	18.9
2 θ /deg	5–50	5–60	5–50	5–55	5–55	5–50
diffractometer	AFC5R	AFC5R	AFC5R	AFC5R	AFC5R	AFC5R
no. of data collected	5600	4451	2054	4785	4106	1755
no. of data with <i>I</i> > 3 σ (<i>I</i>)	3224	2088	1770	1286	2285	1158
no. of variables	355	208	206	179	172	140
isotropic refinement	H1–9	C11–56	C5–9		H1–8b	
<i>R</i>	0.044	0.057	0.078	0.098	0.036	0.029
<i>R</i> _w	0.047	0.056	0.059	0.076	0.029	0.025

was stirred for 30 min, the volatiles were removed under reduced pressure. The residue was extracted with ether and passed through an alumina plug. Crystallization from Et₂O–hexanes gave **4q** (275 mg, 0.59 mmol, 58% yield) as yellow-orange crystals. Anal. Calcd for C₂₇H₁₉O₂FFe: C, 69.57; H, 4.08; F, 4.08. Found: C, 69.56; H, 4.06; F, 4.16.

Reaction of 1 with NaSPH. To a CH₂Cl₂ solution (20 mL) of **1** (454 mg, 1.02 mmol) cooled at –78 °C was added NaSPH (132 mg, 1.00 mmol) as a solid in one portion. Then the cooling bath was removed, and the mixture was gradually warmed to ambient temperature. After the mixture was stirred for 1 h, the volatiles were removed under reduced pressure. The residue was extracted with ether and passed through an alumina plug. Crystallization from nitromethane gave **4t** (402 mg, 0.86 mmol, 86% yield) as yellow-orange crystals. Anal. Calcd for C₂₇H₂₀O₂SFe: C, 69.84; H, 4.34; S, 6.91. Found: C, 69.68; H, 4.34; S, 6.61.

Reaction of 2 with NH₂Prⁱ. To a CH₂Cl₂ solution (40 mL) of **2** (702 mg, 2.03 mmol) cooled at –78 °C was added NH₂Prⁱ (2.0 mL, 34 mmol). Then the cooling bath was removed, and the mixture was gradually warmed to ambient temperature. During this period, the solution color changed from orange to dark brown. After the mixture was stirred for 10 min, the volatiles were removed under reduced pressure. The residue was extracted with ether and passed through an alumina plug. Crystallization from hexanes gave **10a** (246 mg, 0.78 mmol, 38% yield) as dark brown crystals. Anal. Calcd for C₁₆H₂₃NO₂Fe: C, 60.58; H, 7.31; N, 4.42. Found: C, 59.57; H, 7.21; N, 4.15. From the residue, which was insoluble in ether, the cationic amine complex **11a** was isolated as a black solid.

Reaction of 2 with NHPriⁱ. To a CH₂Cl₂ solution (20 mL) of **2** (355 mg, 1.03 mmol) cooled at –78 °C was added NHPriⁱ (1.0 mL, 7.1 mmol). Then the cooling bath was removed, and the mixture was gradually warmed to ambient temperature. During this period, the solution color changed from orange to yellow. After the mixture was stirred for 1 h, the volatiles were removed under reduced pressure. The residue was extracted with hexanes and passed through an alumina plug. Removal of the volatiles under reduced pressure left **12** (184 mg, 0.71 mmol, 69% yield) as a yellow oil. **12**: δ_H (C₆D₆) 1.25 (3H, t, CH₂CH₃), 1.72 (3H, d, CHCH₃), 2.06–2.19 (2H, m, CH₂CH₃), 4.13 (5H, s, Cp), 4.7 (1H, m, =CH); δ_C (C₆D₆) 15.6, 15.7 (q × 2, J = 126 Hz, CH₃), 36.6 (t, J = 178 Hz, CH₂), 76.1 (d, 160, =CH), 85.6 (d, J = 180, Cp), 87.9 (s, C_o), 200.3 (m, C_β), 216.5, 216.7 (s × 2, CO). IR (CH₂Cl₂): ν_{CO} 2013, 1957 cm⁻¹. An analytically pure sample of oily **12** could not be obtained.

Reaction of 2 with NaSEt. To a CH₂Cl₂ solution (40 mL) of **1** (711 mg, 2.05 mmol) cooled at –78 °C was added NaSEt (277 mg, 3.30 mmol) as a solid in one portion. Then the cooling bath was removed, and the mixture was gradually warmed to ambient temperature. After the mixture was stirred for 30 min, the volatiles were removed under reduced pressure. The residue was extracted with ether and passed through an alumina plug. Crystallization from CH₂Cl₂–hexanes gave Fp-SEt (152 mg, 0.64 mmol, 31% yield). Chromatographic separation of the mother liquor gave two yellow bands, from which the two metallacyclic compounds were isolated: **14i** (eluted with CH₂Cl₂/hexanes = 1:5; recrystallized from hexanes 107 mg, 0.33 mmol, 16% yield) and **15i** (eluted with CH₂Cl₂/hexanes = 1:3; 153 mg, 0.47 mmol, 23% yield). Further chromatographic separation of the mother liquor of **14i** gave **16i** (165 mg, 0.52 mmol, 25% yield) as a yellow oil.

Other reactions were carried out with essentially the same methods as described above.

Experimental Procedure for X-ray Crystallography. Suitable single crystals were mounted on glass fibers, and diffraction measurements were made on Rigaku AFC-5, AFC-5R, and AFC7R automated four-circle diffractometers by using graphite-monochromated Mo K α radiation ($\lambda = 0.71059 \text{ \AA}$). The unit cells were determined and refined by a least-squares method using 20 independent reflections ($2\theta \approx 20^\circ$). Data were collected with an ω – 2θ or ω -scan techniques. If $\sigma(F)/F$ was more than 0.1, a scan was repeated up to three times, and the results were added to the first scan. Three standard reflections were monitored at every 100 (AFC5) and 150 measurements (AFC5R and AFC7R). Data collections were performed on a FACOM A-70 (data collection by AFC5), a micro vax II computer (data collection by AFC5R), and a VENTURIS FX 5133 computer (data collection by AFC7R), and structural analysis was performed on IRIS Indigo and O2 computers (structure analysis) by using the teXsan structure solving program system³⁶ obtained from the Rigaku Corp., Tokyo, Japan. Neutral scattering factors were obtained from the standard source.³⁷ In the reduction of data, Lorentz and polarization corrections were made. An empirical absorption correction (Ψ scan) was also made. Crystallographic data and the results of refinements are summarized in Table 4.

The structures were solved by a combination of the direct methods (SAPI91³⁸ and MITHRIL³⁹) and Fourier synthesis (DIRDIF).⁴⁰ Unless otherwise stated, non-hydrogen atoms were refined with anisotropic thermal parameters, and hydrogen atoms were fixed at calculated positions (C–H = 0.95 Å) and were not refined. In case the number of diffraction data was not enough for full refinement, some atoms were refined with isotropic parameters (**4o** and **4y**) or using rigid groups (C22–26 in **4o**; C11–15 in **11c**; C5–9 in **13f**), as indicated in Table 4. The disordered BF₄ groups (B2 and F5–8 in **1** and **2**) were also refined using rigid groups, and the population of the two disorder components in **2** was found to be B1F1–4:B2F5–8 = 1:1.

Acknowledgment. We are grateful to the Yamada Science Foundation and the Ministry of Education, Culture, Sports, Science and Technology of the Japanese Government for financial support of this research.

Supporting Information Available: Tables of spectroscopic data for organometallic products and the results of elemental analyses. Tables of positional parameters and B_{eq} values, anisotropic thermal parameters, bond lengths and angles, and atomic numbering schemes. This material is available free of charge via the Internet at <http://pubs.acs.org>.

OM010095T

(36) *teXsan; Crystal Structure Analysis Package*; Rigaku Corp.: Tokyo, Japan, 1985, 1992, and 1999.

(37) *International Tables for X-ray Crystallography*; Kynoch Press: Birmingham, 1975; Vol. 4.

(38) Fan, H.-F. *Structure Analysis Programs with Intelligent Control*; Rigaku Corp.: Tokyo, Japan, 1991.

(39) Gilmore, C. J. *MITHRIL—an integrated direct methods computer program*; University of Glasgow: Glasgow, UK, 1990.

(40) Beurskens, P. T.; Admiraal, G.; Beurskens, G.; Bosman, W. P.; Garcia-Granda, S.; Gould, R. O.; Smits, J. M. M.; Smykalla, C. *The DIRDIF program system. Technical Report of the Crystallography Laboratory*; University of Nijmegen: Nijmegen, The Netherlands, 1992.